Task 1.1

Title

Resource exploration and characterization

Projects (presented on the following pages)

Searching for microseismicity in the Great Geneva basin and surrounding regions
Verónica Antunes, Thomas Planès, Riccardo Minetto, Aurore Carrier, François Martin, Michel Meyer, Matteo Lupi

Mechanical response of Opalinus Clay during CO_2 injection
Alberto Minardi, Lyesse Laloui

Computerized tomography imaging of fracture aperture distribution and fluid flow within sheared fractures
Quinn C. Wenning, Claudio Madonna, Ronny Pini, Takeshi Kurotori, Claudio Petrini, Sayed Alireza Hosseinzadeh Hejazi

Effects of thermal stresses on rocks physical properties: Insights for monitoring at the field scale
Lucas Pimienta, Marie Violay

Seismic activity caused by drilling in supercritical conditions in the Larderello geothermal field
Riccardo Minetto, Domenico Montanari, Thomas Planès, Marco Bonini, Chiara del Ventisette, Matteo Lupi

Estimation of fracture normal compliance from full-waveform sonic log data
Nicolás D. Barbosa, Eva Caspari, J. Germán Rubino, Andrew Greenwood, Ludovic Baron, and Klaus Holliger

Ambient seismic noise tomography of the Geneva basin
Thomas Planès, Anne Obermann, Veronica Antunes, Aurore Carrier, Matteo Lupi

Data acquisition and numerical modeling for a thermally induced breakout experiment
Arnaud Rüegg, Reza Sohrabi, Benoît Valley

Penetration depth of meteoric water and maximum temperatures in orogenic geothermal systems
Larryn W. Diamond, Christoph Wanner, H. Niklaus Waber

How can the borehole three-dimensional displacement data help improving in situ stress estimation across a fault reactivated by fluid injections?
Maria Kakurina, Yves Guglielmi, Christophe Nussbaum and Benoît Valley

Estimating fracture apertures and related parameters using tube-wave data
Jürg Hunziker, Andrew Greenwood, Shohei Minato, Eva Caspari and Klaus Holliger

Characterization of the fracture network in the damage zone of a shear fault with geophysical borehole methods
Eva Caspari, Andrew Greenwood, Ludovic Baron, Daniel Egli, Enea Toschini and Klaus Holliger

Attenuation and velocity anisotropy of stochastic fracture networks
Eva Caspari, Jürg Hunziker, Marco Favino, German Rubino, Klaus Holliger

Seismic attenuation and P-wave modulus dispersion in poroelastic media with fractures of variable aperture distributions
Simon Lissa, Nicolas Barbosa, German Rubino and Beatriz Quintal

GEOTHEST - Building an INTERREG project France-Switzerland on innovation in geophysical exploration for geothermal development in sedimentary basin.
Guillaume Mauri, Jean-Luc Got, Matteo Lupi, Emmanuel Trouver , Andrew Stephen Miller

Reactive transport models of the orogenic hydrothermal system at Grimsel Pass, Switzerland
Peter Alt-Epping, Larryn W. Diamond, Christoph Wanner

Compilation of data relevant for geothermal exploration – a first step towards a Geothermal Play Fairway Analysis of the Rhône Valley
DB van den Heuvel, S Mock, D Egli, LW Diamond, M Herwegh

In-situ characterization of fluid flow In an EGS analog reservoir
Bernard Brixel, Maria Klepikova, Mohammadreza Jalali, Clément Roques, Clément, Simon Loew

Salt Tracer Flow Path Reconstruction Using Ground Penetrating Radar
Peter-Lasse Giertzuch, Joseph Doetsch, Mohammadreza Jalali, Alexis Shakas, Hannes Krietsch, Bernard Brixel, Cédric Schmelzbach, Hansruedi Maurer

Comparison between DNA nanotracer and solute tracer tests in a fractured crystalline rock – GTS case study
Anniina Kittilä, Mohammedreza Jalali, Keith Frederick Evans, Xian-Zhao Kong, Martin O. Saar

GECOS: Geothermal Energy Chance Of Success
Luca Guglielmetti, Andrea Moscariello, Cédric Schmelzbach, Hansrued Maurer, Carole Nawratil de Bono, Michel Meyer, Francois Martin, David Dupuy, PierVittorio Radogna

Exploring the interface between shallow and deep geothermal systems: the Tertiary Molasse.
Andrea Moscariello, Nicolas Clerc, Loic Pierdona, Antoine De Haller

Processing and Analysis of Gravity data across the Geneva Basin in a Geothermal Perspective
Luca Guglielmetti, Andrea Moscariello

SCCER-SoE Annual Conference 2018

Searching for microseismicity in the Great Geneva basin and surrounding regions

Verónica Antunes[1], Thomas Planès[1], Riccardo Minetto[1], Aurore Carrier[1], François Martin[2], Michel Meyer[2], Matteo Lupi[1]

1) Department of Earth Sciences, University of Geneva, Switzerland (veronica.antunes@unige.ch); 2) Services Industriels de Genève - SIG, Switzerland

SCCER SoE
SWISS COMPETENCE CENTER for ENERGY RESEARCH
SUPPLY of ELECTRICITY

Supported by:
Schweizerische Eidgenossenschaft
Confédération suisse
Confederazione Svizzera
Confederaziun svizra

Swiss Confederation

Innosuisse – Swiss Innovation Agency

INTRODUCTION

Switzerland is promoting the development of renewable energetic resources. In particular, the Canton of Geneva and the Industrial Services of Geneva (SIG) are investigating the geothermal energy potential of the Greater Geneva Basin, Western Switzerland. Before exploration starts it is crucial to study the local seismicity and its relationship with local tectonic structures. Additionally, it is important to monitor the seismic activity that may occur during geothermal exploitation.

Background seismicity

Before 1975 | After 1975

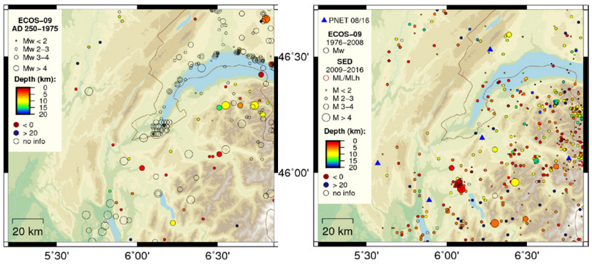

SED (Swiss Seismological Service) catalogues for the Greater Geneva Basin and surrounding area from AD 250 to August 2016 [1].

Historical Seismicity

> Several earthquakes documented in Geneva

Instrumental Seismicity

> Sparce and disperse seismic activity

Number of Stations ?

We installed 20 broadband stations (UG)

WORKFLOW

RAW DATA → CONVERSION → **MSEED** → LASSIE [2] → **DETECTIONS** → SEISAN [3] → **IDENTIFICATION AND LOCATION** → OBSPY [4] → **MAGNITUDE** → **SEISMIC CATALOGUE**

Distance attenuation function: Kradolfer (1984) [5]

$$M_L = \log(A_{WA}) + 0.0180 \cdot D + 1.77 \quad \text{for } D \leq 60 \text{ km}$$
$$M_L = \log(A_{WA}) + 0.0038 \cdot D + 2.62 \quad \text{for } D > 60 \text{ km}$$

1D Velocity Model: Husen et al. (2003) [6]

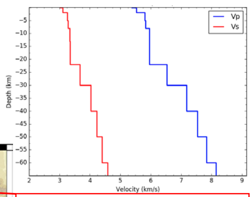

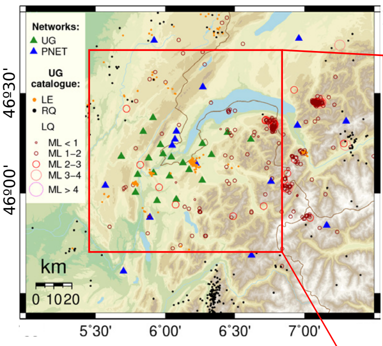

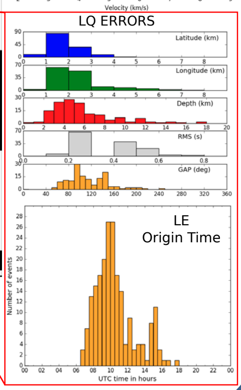

Stations from the permanent network:
FR [7]: OG02, OG35, OGMY, OGSI, OGSM, OGRV, RIVEL, RSL; **CH** [8]: AIGLE, BRANT, GIMEL, SENIN, TORNY; **GU** [9]: REMY; **C4** [10]: CERN1, CERN5, CERNS

SEISMICITY

17 months

LASSIE - 1734 detections:
- 362 Local earthquakes (LQ)
  143 in the area of study
- 218 Quarry blasts (LE)
- 853 Regional (RQ)
- 218 Distant (DQ)
- 83 False detections (F)

1 month (June):
104 real events
STA/LTA - 2097 detections
LASSIE - 124 detections

LASSIE detection: 2017-06-02 02:04 ML 1.1

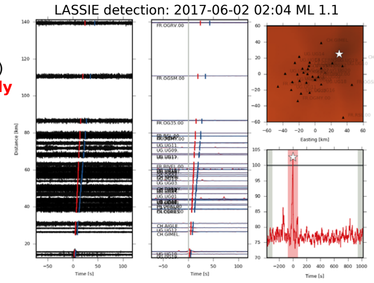

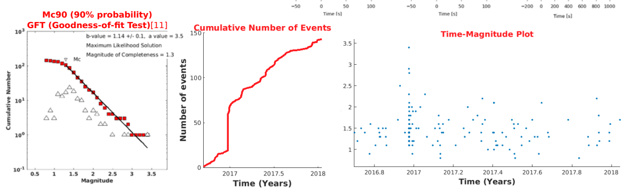

Mc determined using GISMO [12]: we think the Mc value is being overestimated due the low seismic rate in the area; Evolution of events through time, SEDA [13]: the seismic sequence that occurred in December 2016 is evident.

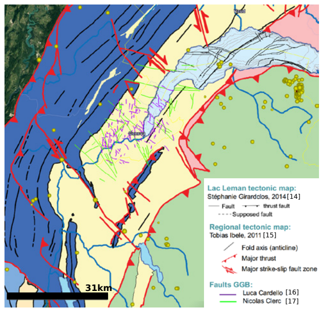

UG catalogue and Tectonic Map of the region

01/09/2016 - 31/01/2018
143 LQ UG catalogue
44 LQ Swiss catalogue
14 LQ French catalogue

Seismogenic areas:
- Vuache fault
- Lake Leman
- NE of the basin (Pre-Alpine front)
- Arve fault
- Isolated events indicating disperse seismicity

Seismic rate:
17months/143 events
1year/~100 events

MONITORING

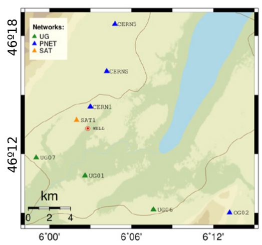

One extra station deployed near the Satigny well

01/01/2018 - 03/05/2018
0 events

We developed a tool capable to locate unconventional events. The method is based on the **back-projection** of the **cross-correlation envelope** [18] [19] of signals between **pairs of stations**.

SIGNAL PROCESSING (Remove mean, trend and instrument response, filter, normalizing, and amplitude weight factor) → **2D GRID** → **CROSS-CORRELATION ENVELOPE** (Between pairs of stations for each time segment) → **DIFFERENTIAL TRAVEL-TIME** (From each grid point to each station pair) → **INDIVIDUAL BACK-PROJECTIONS** (For each station pair: using the differential time from each grid point to get the envelope) → **STACK AND NORMALIZATION** → **RELOCATION SOLUTION** (Plotted as a colored 2D map)

Successfully applied to locate seismic signals associated with geothermal activity [20]

UNIVERSITÉ DE GENÈVE
FACULTÉ DES SCIENCES

Acknowledgments:
SIG (Services Industriels de Genève) that are financing this study; All land-owners that hosted the seismic stations; Sebastian Heimann and Simone Cesca that hosted me for more than one week at the GFZ institute, in Potsdam and provided me support with LASSIE; Catarina Matos, that first sugested me to use LASSIE and for all feedback and suggestions.

REFERENCES:
[1] Fäh, D. et al. (2011) DOI: SED/RISK/R/001/20110417; [2] Heimann S. et al. (in prep.); [3] Havskov and Ottemoller (1999) http://seisan.info; [4] Beyreuther M. (2010) DOI: 10.1785/gssrl.81.3.530; [5] Kradolfer, U. (1984), Diploma thesis. ETH Zurich; [6] Husen S., et al. (2003) DOI: 10.1029/2002JB001778; [7] RESIF (1995) DOI: 10.15778/RESIF.FR; [8] SED (1983) DOI: 10.12686/sed/networks/ch; [9] University of Genova (1967) DOI: 10.7914/SN/GU; [10] CERN Seismic Network, C4 (2017); [11] Wiemer, S. et al. (2000) DOI: 10.1785/0119990114; [12] Thompson G and Reyes C. (2017) http://geoscience-community-codes.github.io/GISMO; [13] A. M. Lombardi (2017) DOI: 10.1038/srep44171; [14] Girardclos S. et al (2014), 19º congrés international de sédimentologie; [15] Ibele T. (2011) PhD thesis; [16] Cardello L., et al. EGU 2017 poster presentation; [17] Clerc N., et al., Proceedings World Geothermal Congress 2015; [18] Shapiro et al. (2006) DOI:10.1029/2006GL027010; [19] Ballmer et al. (2013) DOI: 10.1093/gji/ggt112; [20] Minuetto et all, EGU 2018, Oral presentation.

SIG

lassie

SCCER SoE
SWISS COMPETENCE CENTER for ENERGY RESEARCH
SUPPLY of ELECTRICITY

SCCER-SoE Annual Conference 2018

Supported by:
Schweizerische Eidgenossenschaft
Confédération suisse
Confederazione Svizzera
Confederaziun svizra
Swiss Confederation
Innosuisse – Swiss Innovation Agency

Mechanical response of Opalinus Clay during CO_2 injection

Alberto Minardi and Lyesse Laloui
École Polytechnique Fédérale de Lausanne - EPFL

Introduction and motivations

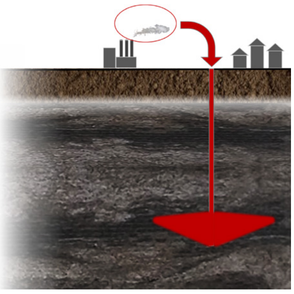

Research of the chair "Gaz Naturel" – Petrosvibri at the EPFL contributes to SCCER-SoE WP1: "DGE and CO_2 sequestration". WP1 research focuses on problems for future realization of CO_2 storage in Switzerland. The deployment of this technology might play a key role in the future for the de-carbonization of fossil energy sources.

The sound characterization of reservoirs and caprocks in Switzerland and the assessment of their potential for CO_2 sequestration is therefore fundamental. In order to grant a safe injection of CO_2 into reservoir formations, the overlaying shaly caprock must perform efficiently.

Objectives:
The research activities deal with the assessment of the hydro-mechanical behavior of the Opalinus Clay shale for a safe geological sequestration of carbon dioxide and the identification of the relevant processes related to CO_2 interactions. In particular the presented study focuses on the experimental evaluation of the sealing capacity of the Opalinus Clay shale during CO_2 injection tests for a better quantification of the capillary entry-pressure of the material.

Experimental set-up

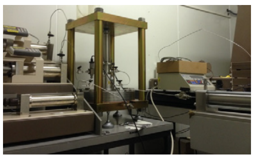

High pressure oedometric cell
- oedometric conditions (no lateral strain)
- water and CO_2 injection under constant stress
- axial LVDTs to monitor displacements

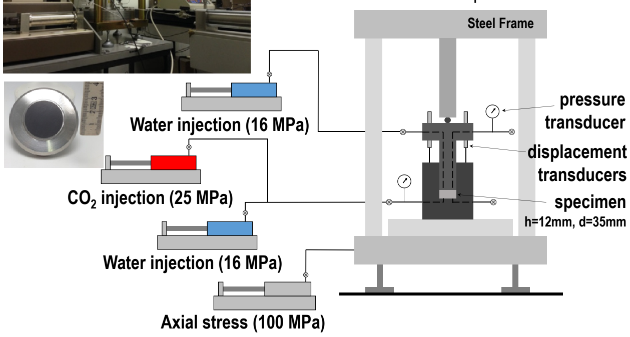

Testing layout and material

- CO_2 is injected at the upstream side (bottom of the sample) in steps
- a constant volume reservoir is connected at downstream side
- CO_2 pressure variations are monitored at the downstream side
- Shaly Opalinus Clay from Mont Terri URL is tested

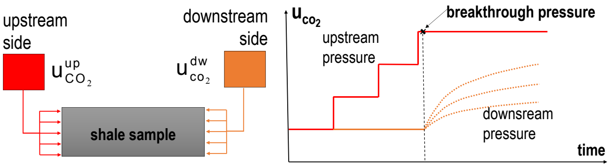

Experimental protocol

1) Samples resaturation with water at constant volume
2) Assessment of the hydraulic condictivity (steady state method)
3) Consolidation to a target effective stress (σ_a=24 MPa, u_w=2 MPa)
4) Initial CO_2 injection at 2 MPa both upstream and downstream side
5) CO_2 injection pressure increased at upstream in steps (4, 8, 12 MPa)
6) CO_2 injection pressure decreased at upstream side to 8 MPa
7) Sample desaturation with free air exposure
8) CO_2 injection performed with the same steps of the stages 5 and 6

Experimental results

CO_2 injection in water saturated sample

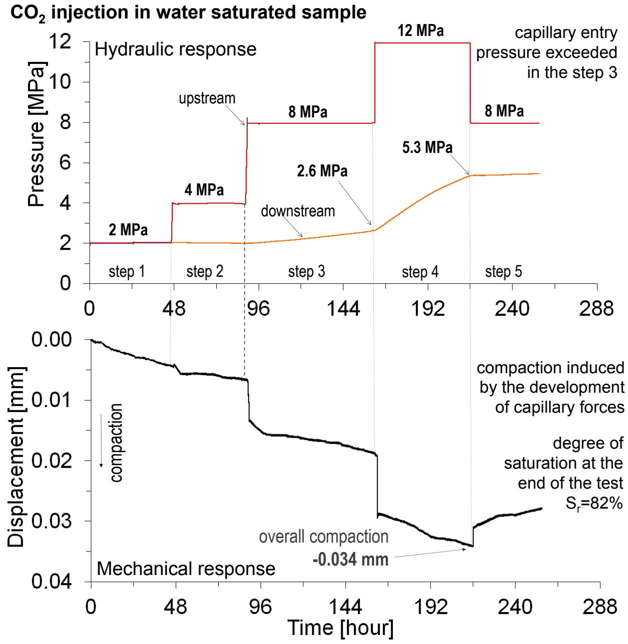

CO_2 injection in unsaturated sample [S_r=37%]

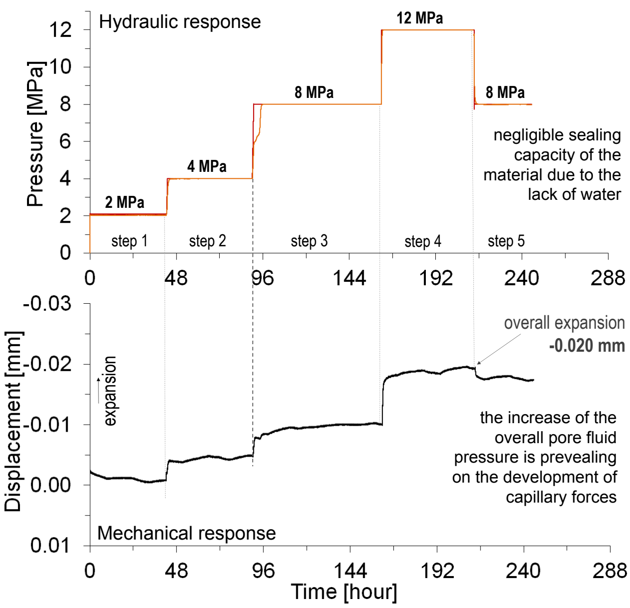

Summary

- experimental methodology to evaluate sealing capacity of shale
- intact Opalinus Clay: capillary entry pressure 2 - 6 MPa
- mechanical response dependent on water saturation
- compaction exhibited during injection in saturated sample

The financial support of Swisstopo is acknowledged

- Favero V, Laloui L. (2018) Impact of CO 2 injection on the hydro-mechanical behaviour of a clay-rich caprock. International Journal of Greenhouse Gas Control. 30(71):133-41.
- Makhnenko RY, Vilarrasa V, Mylnikov D, Laloui L. (2017) Hydromechanical aspects of CO2 breakthrough into clay-rich caprock. Energy Procedia. 1(114):3219-28.

70 NRP Energy Turnaround National Research Programme

SCCER-SoE Annual Conference 2018

SCCER SoE
SWISS COMPETENCE CENTER for ENERGY RESEARCH
SUPPLY of ELECTRICITY
Supported by:
Schweizerische Eidgenossenschaft
Confédération suisse
Confederazione Svizzera
Confederaziun svizra
Swiss Confederation
Innosuisse – Swiss Innovation Agency

Computerized tomography imaging of fracture aperture distribution and fluid flow within sheared fractures

Quinn Wenning[1], Claudio Madonna[1], Takeshi Kurotori[2], Claudio Petrini[1], Sayed A. Hosseinzadeh Hejazi[2], and Ronny Pini[2]

[1]Department of Earth Sciences, ETH Zurich, [2]Department of Chemical Engineering Imperial College London

1. Introduction

- Knowledge of fracture (aperture) distribution is paramount for sound description of fluid transport in low-permeability rocks.
- In the context of geothermal energy development, quantifying the transport properties of fractures is needed to quantify the rate of heat transfer and optimize the engineering design of the operation.
- Core-flooding experiments coupled with non-invasive imaging techniques (e.g., X-Ray Computed Tomography – X-Ray CT) represent a powerful tool for making direct observations of these properties under representative geologic conditions.
- We coupled the CT imaging with a direct shear apparatus to understand the evolution of fracture aperture with displacement on Westerly granite and Carrara marble.

2. Sample preparation and direct shear core-holder

- A single fracture along the Westerly granite and Carrara marble samples was induced via a modified Brazilian test with pointed wedged spacers placed along the top and bottom of the sample.
- Imaging of the fractured sample undergoing direct shear displacement is made possible by a novel X-ray transparent core-holder that was developed and built in-house at ETH Zurich.

Core holder

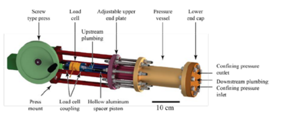

Sample & Spacer

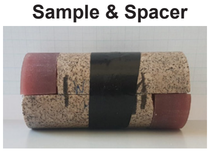

Pressure vessel

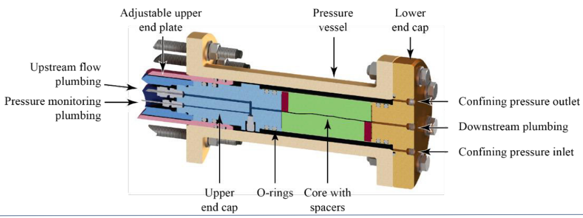

3. Computed tomography methods

- Fracture aperture estimation follows the calibration free missing attenuation method [Huo et al., 2016].
- CT number in the vicinity of a fracture will be reduced due to density deficiency in the gas filled fracture.
- Smearing of the X-ray attenuation due to partial volume effects will cause lower CT numbers adjacent to the fracture.
- Main assumption is that all X-ray attenuation is conserved and that the real CT value of the un-fractured rock can be estimated by neighboring voxels.

Whole core CT image

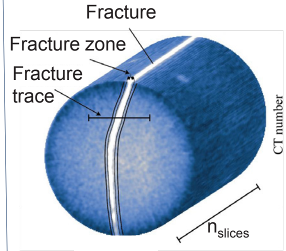

Fracture trace

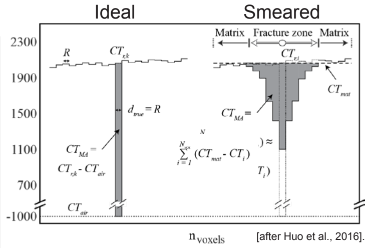

$$d = \frac{R \cdot \sum_{i=1}^{N_{vox}} (CT_{mat} - CT_i)}{CT_{mat} - CT_{gas}}$$

4. Results

Aperture maps: Westerly granite

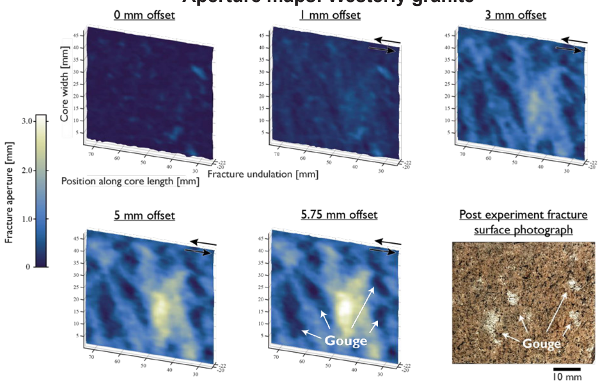

Aperture distribution

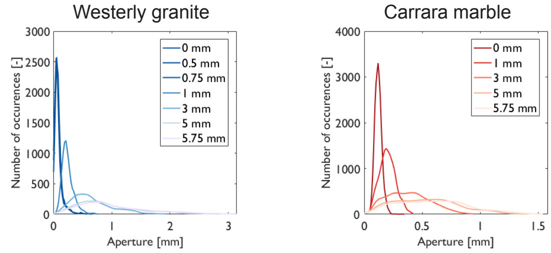

Mean aperture

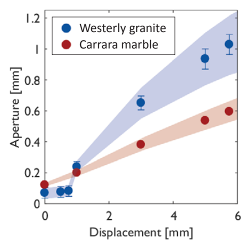

Joint roughness coefficient

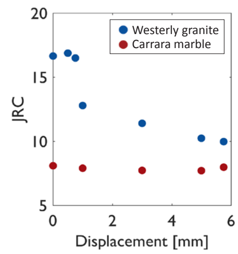

Aperture maps: Carrara marble

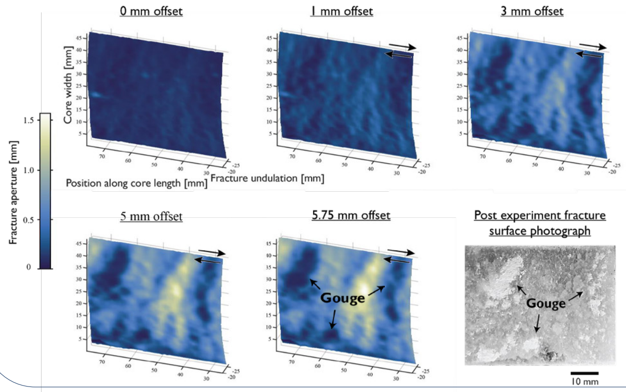

5. Conclusions

- We are able to directly image and calculate fracture aperture using CT imaging
- Aperture increases and develops anisotropy with shearing.
- Roughness controls aperture evolution with shearing.
- Minima changes in aperture are expected for (stimulation induced) earthquakes less than ~ 1 M.

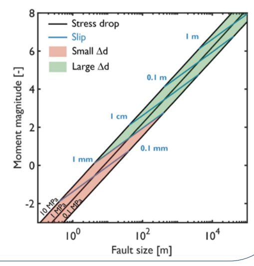

Special thanks to: Thomas Mörgeli for fabrication of the core-holder, the SASEG Student Grant for partial funding of the core-holder.

Reference: Huo et al., 2016. A calibration-free approach for measuring fracture aperture distributions using X-ray computed tomography. Geosphere, v. 12, no. 2.

SCCER SoE
SWISS COMPETENCE CENTER for ENERGY RESEARCH
SUPPLY of ELECTRICITY

ÉCOLE POLYTECHNIQUE FÉDÉRALE DE LAUSANNE

SCCER-SoE Annual Conference 2018

Supported by:
Schweizerische Eidgenossenschaft
Confédération suisse
Confederazione Svizzera
Confederaziun svizra

Swiss Confederation

Innosuisse – Swiss Innovation Agency

European Commission

Effects of thermal stresses on rocks physical properties
Insights for monitoring at the field scale

Lucas Pimienta & Marie Violay
Laboratory of Experimental Rock Mechanics, EPFL, Lausanne, Switzerland

Motivation:

Field seismic and electrical resistivity are powerful tools to investigate from the surface geological reservoir rocks at depth.

The two methods are complementary and have been largely used to prospect for oil/gas reservoirs. However, little is still known on the intrinsic dependences of the two properties to the degree of microfracturation (e.g. Pimienta et al., 2017). Moreover, electrical properties have seldom been measured in the high pressure and high temperature range (Violay et al., 2012)

Using thermal treatment at different temperatures, known to induce a variable degree of microfracturation in rocks (e.g. Nasseri et al., 2007), the aim of this work is to investigate how the degree of microfracturation affects the physical properties of rocks at both the laboratory and the field scale (e.g. Pimienta et al., 2016).

Project:

- ***PROGRESS:*** *PROspection and PROduction of Geothermal RESServoirS*
- Understand the links between physical properties in geothermal reservoir rocks.

Samples & Methods:

➢ Approach: Evolution in properties for varying degree of damage
⇒ Thermal treatment in oven for T in the range of [20,1000] °C

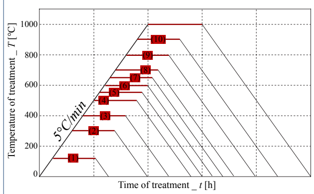

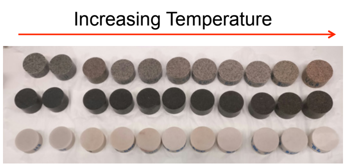

➢ Rocks samples: (11 for each rock)
- **Marble** (Carrara) : ϕ = [0.1;0.3]% // 0% quartz
- **Diorite** : ϕ = [0.1;0.3]% // Approx. 30 % quartz
- **Granite** (Westerly) : ϕ = [0.7;1.3]% // Approx. 30 % quartz
- **Sandstones**
  - FoS4 (Fontainebleau): ϕ = [3.8;4.3]% // 100% quartz
  - FoS6 (Fontainebleau): ϕ = [5.8;6.3]% // 100% quartz

➢ Petrophysical characterisation:
- ➢ Pore & Bulk volumes
- ➢ P- & S-wave velocities (frequency of 1 MHz)
- ➢ Electrical impedance (frequency from 0.1 Hz to 100 kHz)

Results

Bulk & Pore volume variations :

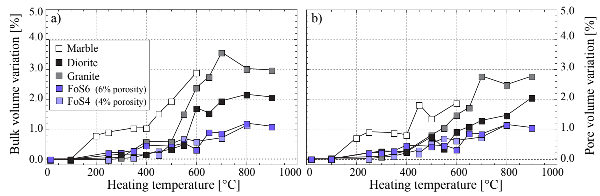

P- and S-wave velocity variations :

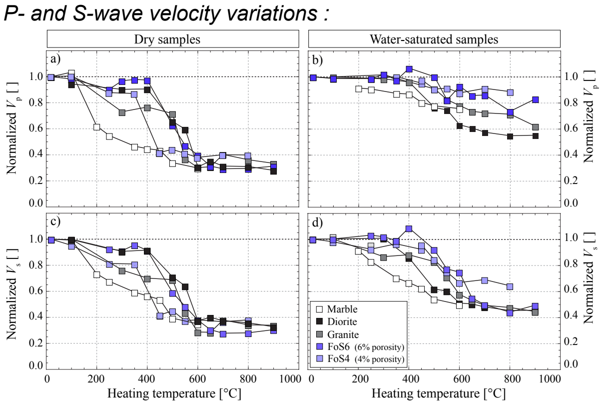

Electrical resistivity variations :

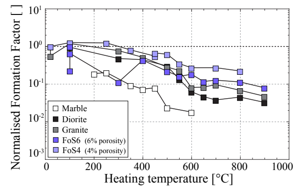

Insights from the electrical impedance measurements :

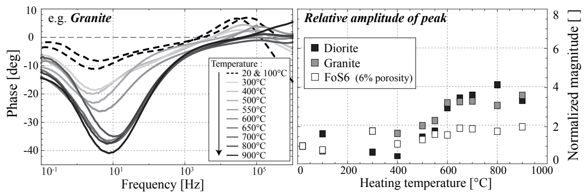

Discussion

Insights on the physics of thermal cracking (lab. scale):

➢ Dramatic effects of the temperature in rocks, even though temperature rate is kept low
⬄ Role of grains anisotropic thermal expansions.
➢ Variable dependence to the temperature for the different properties, and the different rocks.
➢ V_p => Crack density => Comparison between transport properties:

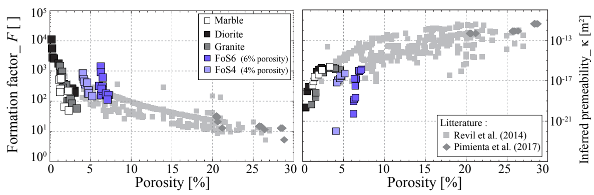

Insights for the field scale

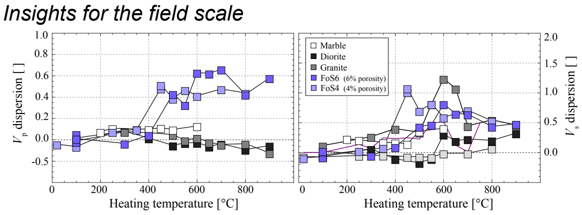

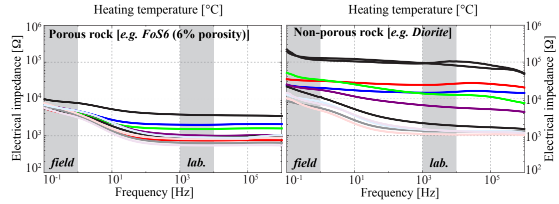

Elastic ⬄ Strong effects in porous rocks, Little in non-porous ones
Transport ⬄ Little effects in porous rocks, Strong in non-porous ones

References

- Nasseri, M. H. B., Schubnel, A., & Young, R. P. (2007). Coupled evolutions of fracture toughness and elastic wave velocities at high crack density in thermally treated Westerly granite. *International journal of rock mechanics and mining sciences*, *44*(4), 601-616.
- Pimienta L., Sarout, J., Esteban, L., David, C., & Clennell, B. (2017): Pressure-dependent elastic and transport properties of porous and permeable rocks: Microstructural control, *Journal of Geophysical Research*, **122**(11), 2169-9356.
- Violay, M., Gibert, B., Azais, P., Pezard, P. A., & Lods, G. (2012): A new cell for electrical conductivity measurement on saturated samples at upper crust conditions, *Transport in porous media*, **91**(1), 303-318.
- Pimienta, L., Fortin, J., Borgomano, J.V.M., & Guéguen, Y. (2016): Dispersions & Attenuations in a fully saturated sandstone: Experimental evidence for fluid flows at different scales, *The Leading Edge*, **35**(6), 495-501.

Seismic activity caused by drilling in supercritical conditions in the Larderello geothermal field

Riccardo Minetto[1], Domenico Montanari[2], Thomas Planès[3], Marco Bonini[2], Chiara del Ventisette[4] and Matteo Lupi[3]

[1] University of Trieste, Italy. [2]National Research Council of Italy, [3]University of Geneva, Switzerland, [4]University of Florence, Italy,

Introduction

Supercritical fluids (T > 374°C and $P > 210$ bar) are an economically attractive resource thanks to their high power-producing potential.
One of the most recent attempt to reach supercritical fluids took place in 2017 at the Larederello-Travale geothermal field (LTGF), Italy, with the deepening of the Venelle 2 well. The well did not find supercritical fluids but $T > 500$°C were measured at 2900 m [1]. To monitor the seismic activity of the ongoing well we deployed 8 seismic stations around the drilling site.

Seismic network

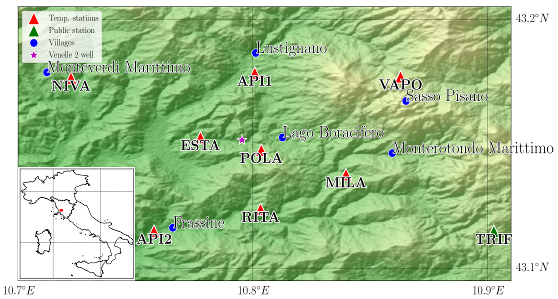

Figure: Map of the study area showing the employed seismic network composed of 9 broadband stations and active from June 2017 to January 2018.

- Acquisition period: 23 June 2017 - 21 January 2018.
- Stations: 8 temporary and 1 permanent (INGV network).
- Instruments: Trillium Compact sensors with period of 20 or 120 s and Data-Cube[3] digitizers with sampling frequency of 100 Hz.

Recorded events

On 20 October 2017 the Venelle 2 well experienced a total loss of circulation at 2700 m, with $T > 400$°C and pressure of 300 bar [1]. Few days after and before such date (between 16-18 October and on 24 October 2017) two swarms were detected.
These events have the following features:

- unclear P and S-waves arrivals;
- low amplitude with values decreasing with increasing distance from the well;
- high similarity, but great variability of the waveforms at different stations;
- almost monochromatic frequency content (7-8 Hz);

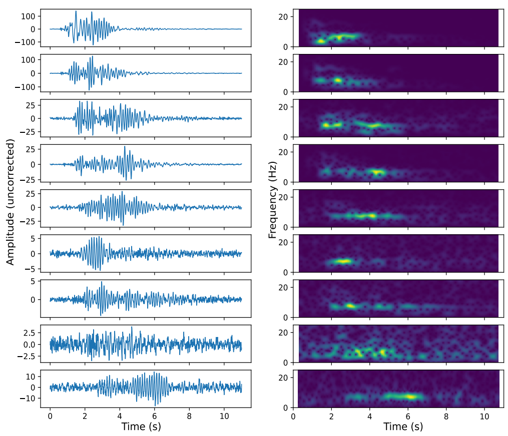

Figure: Seismograms (vertical components) recorded at each station (left) along with the corresponding spectrograms (right).

Temporal evolution

Considering the two swarms, a total of 250 events were distinguished cross-correlating a template and using as threshold a correlation coefficient > 0.8. In both cases the events occurred in groups with an almost periodic occurrence.

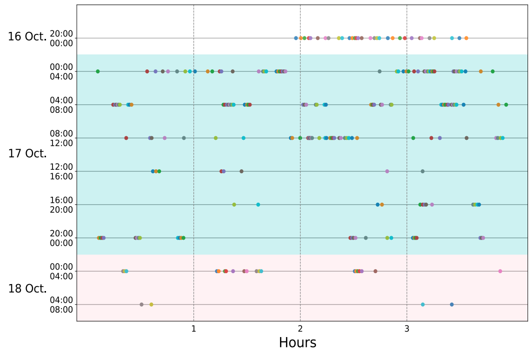

Figure: Temporal evolution of the major swarm recorded from 16 to 18 October 2017. Each dot corresponds to one event (184 in total).

Events location

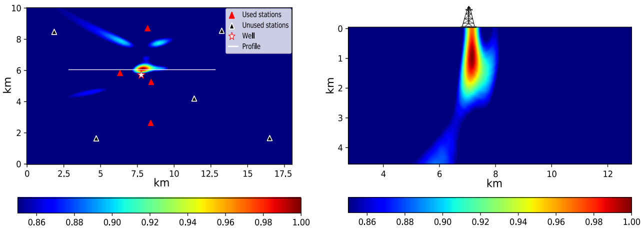

Figure: Swarms location: horizontal slice at 1 km (left) and vertical cross-section (right). The largest values indicate the most likely source location.

The most probable source location has been constrained in the first 2 km below Venelle 2 well. The location was calculated using a method based on cross-correlation [2] supposing a constant velocity of 4 km/s and a straight propagation path.

Discussion and conclusions

- The recorded events have distinctive features reminding LP (low period) events and therefore they may share similar source processes [3], in this case likely related to the presence of geothermal fluids.
- The Venelle 2 well may have played a role in the genesis of the swarms. This theory agrees with the source location of the events, their coincidence with a total loss of circulation and their distinctive characteristics.
- Longer monitoring times may help to understand if the swarms are really related to the well or if they are completely natural expressions in the LGTF.

References

[1] Bertani et al. (2018). The First Results of the DESCRAMBLE Project. 43rd Workshop on Geothermal Reservoir Engineering.

[2] Ballmer at al. (2013). Ambient seismic noise interferometry in Hawaii reveals long-range observability of volcanic tremor. Geophysical Journal International, 194, 512-523.

[3] Sgattoni et al. (2016). Long-period seismic events with strikingly regular temporal patterns on Katla volcano's south flank (Iceland). Journal of Volcanology and Geothermal Research, 324, 28-40.

Contact Information

- Email: minetto.riccardo@gmail.com
- Phone: +39 329 669 8840

SCCER SoE
SWISS COMPETENCE CENTER for ENERGY RESEARCH
SUPPLY of ELECTRICITY

SCCER-SoE Annual Conference 2018

Supported by:
Schweizerische Eidgenossenschaft
Confédération suisse
Confederazione Svizzera
Confederaziun svizra
Swiss Confederation
Innosuisse – Swiss Innovation Agency

Estimation of fracture normal compliance from full-waveform sonic log data

Nicolás D. Barbosa[1], Eva Caspari[1], J. Germán Rubino[2], Andrew Greenwood[1], Ludovic Baron[1], and Klaus Holliger[1]

1- University of Lausanne
2- CONICET, Centro Atómico Bariloche

Introduction

Fractures can have a predominant influence on the mechanical and hydraulic properties of reservoirs. For this reason, the identification and characterization of fractures is of increasing concern in many domains ranging from the development of hydrocarbon and geothermal reservoirs to the geological storage of CO_2 and nuclear waste. Given that seismic waves propagating through fractured rocks are known to be slowed down and attenuated, seismic methods are valuable for characterizing the hydromechanical behaviour of these environments. In this work, we characterize the mechanical properties of individual fractures from P-wave velocity changes and transmission losses inferred from static full-waveform sonic (FWS) log data.

Experimental background

Static FWS data were acquired at the Grimsel Test Site (GTS) INJ2 borehole using a single transmitter and three receivers at nominal source frequencies of 15 and 25 kHz (Figs. 1 and 2).

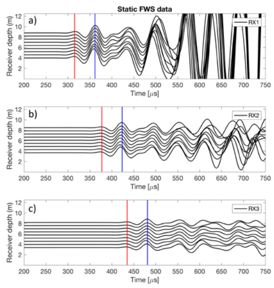

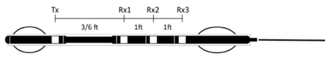

Fig.1: Sonic log tool with one transmitter (Tx) and three receivers (Rx1, Rx2, Rx3). The offset to the source of the first receiver can be 3 or 6 ft.

Fig.2: Static FWS data recorded in the upper section of the borehole for receivers (a) Rx1, (b) Rx2, and (c) Rx3. The red and blue vertical lines illustrate the central time of the time windows employed to isolate one and two cycles of the first P-wave arrival, respectively.

Analysis of phase velocity and attenuation from FWS data

Phase velocity: After isolation of the first-arriving P-wave, we determine phase velocities v_p for each interval between receivers (Fig. 3) from the phase difference $\Delta\varphi$ of the corresponding recorded signals

$$v_p(\omega)=\frac{\omega\Delta r}{\Delta\varphi(\omega)}, \qquad (1)$$

where ω is the angular frequency and Δr the distance between receivers.

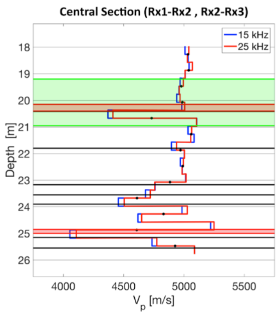

Fig. 3: P-wave velocity for nominal source frequencies of 15 and 25 kHz. The region colored in green corresponds to a shear zone. Horizontal black lines and red layers denote to fractures and dykes, respectively, identified from televiewer images. Notice that fractures can act as planes of mechanical weakness producing significant decreases in the P-wave velocity.

Attenuation: The raw attenuation Q_p^{-1} for a given receiver interval can be computed as

$$Q_p^{-1}(\omega)=\ln\left(\frac{A(\omega,r_i)}{A(\omega,r_{i+1})}\right)\frac{2v_p(\omega)}{\omega\Delta r}, \qquad (2)$$

where $A(\omega,r_i)$ is the P-wave spectrum at the ith receiver. The attenuation in Eq. 2 can be expressed as

$$Q_p^{-1}(\omega)=Q_{sprd}^{-1}(\omega)+Q_{intr}^{-1}(\omega)+Q_{transm}^{-1}(\omega), \qquad (3)$$

where $1/Q_{sprd}$, $1/Q_{intr}$ and $1/Q_{transm}$ refer to attenuation contributions due to geometrical spreading, intrinsic loss of the host rock, and transmission losses associated with the presence of fractures, respectively.

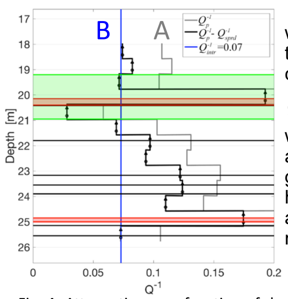

Fig. 4: Attenuation as a function of depth in the central section of the borehole computed from 25 kHz measurements. Black and grey solid curves correspond to attenuation estimates with and without geometrical spreading correction, respectively. The blue vertical line denotes the mean background intrinsic attenuation ($1/Q_{intr}$ in Eq. 3).

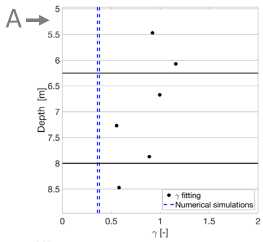

Fig. 5: **Geometrical spreading correction.** Assuming that, in Eq. 3, the geometrical spreading function defining $1/Q_{sprd}$ can be approximated as $G_i=(1/r_i)^{\gamma}$, we use attenuation measurements from different offset configurations (Fig. 1) to estimate the exponent γ. This figure shows γ as a function of depth in the upper section. The blue dashed lines show the range of values of γ estimated from numerical simulations that approximate the borehole environment.

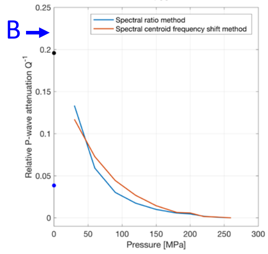

Fig. 6: **Background intrinsic attenuation.** Relative attenuation estimated from ultrasonic measurements (1 MHz) as functions of applied pressure (data from Wenning et al. (2018)). The reference signal corresponds to that at 260 MPa. Core samples are representative of the host rock of the GTS. Blue and orange curves show the attenuation computed using the spectral ratio and centroid frequency shift methods, respectively. The pressure dependence of Q^{-1} suggest the presence of microcracks. We performed ultrasonic measurements on dry (black dot) and water-saturated (blue dot) samples at ambient conditions, the results of which corroborate this hypothesis.

Effect of individual fractures on the attenuation and phase velocity of sonic waves

The increase of attenuation at the fractures in Fig. 4 is related to transmission losses across them ($1/Q_{transm}$). The P-wave transmission coefficient T of a fracture can be computed as

$$T(\omega)=e^{i\left(k_p^b-k_p^{eff}\right)\Delta r}, \qquad (4)$$

and can be linked to its mechanical compliance Z_N through the linear slip theory

$$Z_N=\frac{2(1-T)}{iT\omega I_b}. \qquad (5)$$

In Eqs. 4 and 5, k_p^b and k_p^{eff} correspond to the wavenumbers of the background rock and an effective viscoelastic medium representing the fractured section between two receivers, respectively, and I_b is the background impedance.

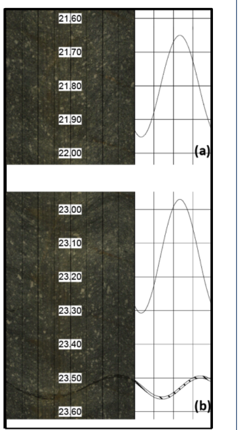

Fig. 7: Televiewer image and its interpretation for the individual fractures in the central section.

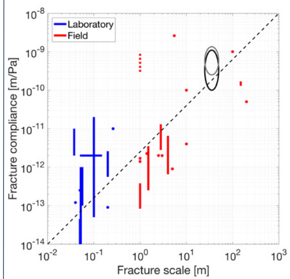

Fig. 8: Laboratory (blue) and field (red) fracture compliance values as function of fracture size compiled from the literature. The black and grey ellipses indicate the range of the real components and absolute values of the compliances reported in this work (Eq. 5).

Conclusions

- In this work, we have analyzed the mechanisms contributing to the sonic P-wave attenuation and velocity observed from static FWS log data from a borehole penetrating granodiorite rocks cut by several discrete fractures.
- We have shown that it is possible to compute the P-wave transmission coefficient associated with the presence of a given fracture from the sonic P-wave attenuation due to transmission losses and the corresponding phase velocity between two receivers.
- Our results indicate that the mechanical compliance of the fractures are likely to lie in the range between 1×10^{-10} m/Pa and 1×10^{-9} m/Pa, which is consistent with the expected values for fractures of the size considered.

Acknowledgements

This work was supported by a grant from the Swiss National Science Foundation and completed within SCCER-SOE with the support of Innosuisse.

SCCER-SoE Annual Conference 2018

UNIVERSITÉ DE GENÈVE

FNS SNF
FONDS NATIONAL SUISSE
SCHWEIZERISCHER NATIONALFONDS
FONDO NAZIONALE SVIZZERO
SWISS NATIONAL SCIENCE FOUNDATION

Ambient seismic noise tomography of the Geneva basin

Thomas Planès, Anne Obermann, Veronica Antunes, Aurore Carrier, Matteo Lupi

Motivation

- The canton of Geneva is currently strongly promoting the development of geothermal energy [1].
- The lack of exploitation of geothermal energy is in part due to the **lack of knowledge of the subsurface geology**.
- Conventional exploration techniques, such as reflection seismics, present **prohibitive costs** for the geothermal energy sector.
- There is a strong need for **affordable exploration methods** at various depths.
- Unconventional exploration techniques such as deep geoelectrics, gravity, and passive seismics are currently being tested in the Great Geneva Basin (GGB).
- In the present work, we present an application of the passive **Ambient seismic Noise Tomography (ANT)** method in the GGB.
- We aim to retrieve a large scale shear-wave velocity model (Vs) of the basin and to evaluate the potential of the technique for geothermal exploration purposes.

Data and methods

- A temporary seismic network composed of 20 stations was deployed from August 2016 to February 2018 in the GGB (Fig. 1).
- This network aims to: (1) study the local micro-seismicity prior to geothermal-related drilling and injection [2], and (2) perform the ANT shown here.
- The noise correlation technique allows to turn a passive receiver (a seismometer) into a virtual source (Fig. 2) [3].

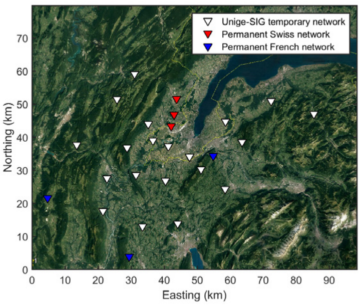

Figure 1: Seismic network used in this study including 20 temporary stations from the University of Geneva (Unige) and the Industrial services of Geneva (SIG), 4 stations from the Swiss permanent network, and 3 stations from the French permanent network.

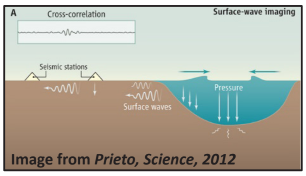

Figure 2: Schematic illustration of the ambient seismic noise generated at the ocean floor and being recorded at two seismometers. Through a cross-correlation process, the surface-wave response between the two stations can be retrieved.

Results

The ANT comprises the following main steps:

- Cross correlation of the noise traces to retrieve the surface wave responses between stations (Fig. 3).
- Picking the group-velocity dispersion curves (Fig. 4).
- Inversion of 2D group-velocity maps at various frequencies using linear least square inversion (Fig. 5).
- Depth inversion using a guided Monte Carlo approach [4] to retrieve the 3D Vs model (Fig. 6).

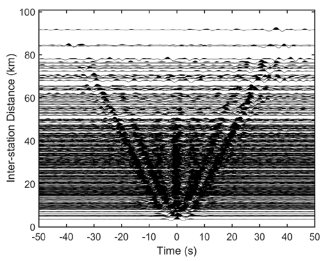

Figure 3: Noise correlation functions ordered by interstation distance showing the retrieval of Rayleigh (surface) waves.

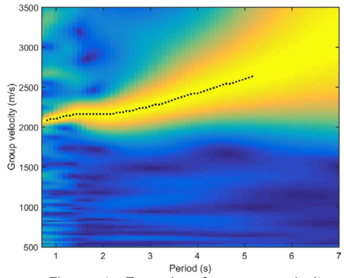

Figure 4: Example of a group-velocity dispersion curve and corresponding picking (dashed line).

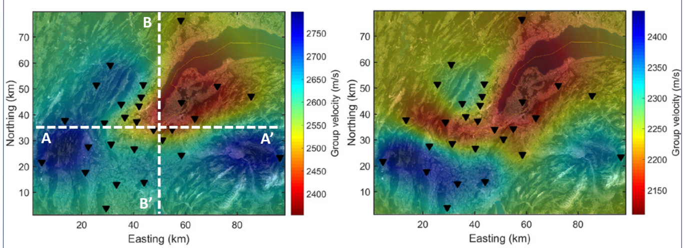

Figure 5: Group velocity maps at periods of 8 s (left) and 4 s (right). A slower velocity (red color) corresponds to softer rocks while a higher velocity (blue color) corresponds to harder rocks. At large periods (eg T=8 s), the velocity pattern is mainly controlled by the basin structure (depth of sediments). At lower periods (eg T=4 s), some observed variations still need to be understood and could be caused by noise-distribution-related biases.

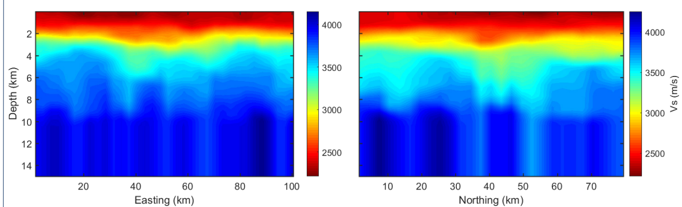

Figure 6: Cross-sections through the retrieved 3D Vs model along profile A-A' (left panel) and along profile B-B' (right panel) marked in Fig. 5. The upper lower-velocity layer in red is related to the geometry of the sedimentary cover.

Discussion and next steps

- Surface wave responses were extracted from ambient seismic noise and allowed to retrieve a large-scale Vs velocity model.
- Eventually, the model will be integrated with other geophysical data to improve our knowledge of the basin.
- Due to the nature of surface waves and to the network "low-density", the retrieved Vs model is not detailed enough for geothermal exploration purposes.

➢ Potential biases induced by a inhomogeneous noise source distribution should be carefully investigated [5].

➢ Deploy a dense network and extract body P- (and S-?) waves from ambient noise [6].

➢ Take advantage of the upcoming 3D active seismic campaign in Geneva to "ground-truth" and further develop the method.

References

[1] http://www.geothermie2020.ch/
[2] see the poster of Veronica Antunes
[3] Campillo and Paul 2003, *Science* ***299****:547-549*
[4] Sambridge 2001, *Inverse problems* ***17****:3*
[5] Lehujeur 2015, *Geothermal energy* ***3****:3*
[6] Nakata 2015, *Journal of Geophysical Research* ***120****(2):1159-1173*

SCCER-SoE Annual Conference 2018

SCCER SoE
SWISS COMPETENCE CENTER for ENERGY RESEARCH
SUPPLY of ELECTRICITY

unine
UNIVERSITÉ DE NEUCHÂTEL

Supported by:
Schweizerische Eidgenossenschaft
Confédération suisse
Confederazione Svizzera
Confederaziun svizra
Swiss Confederation
Innosuisse – Swiss Innovation Agency

DATA ACQUISITION AND NUMERICAL MODELING FOR A THERMALLY INDUCED BREAKOUT EXPERIMENT

Arnaud Rüegg, Reza Sohrabi, Benoît Valley
Centre for Hydrogeology and Geothermics (CHYN), Laboratory of Geothermics and Reservoir Geomechanics, University of Neuchâtel
arnaud.ruegg@unine.ch

Motivation

This research focuses on the thermally induced spalling effect occurring as a result of stress concentration due to excavation in a medium under in-situ stress, combined with thermal expansion of the surrounding material. The Thermally Induced Breakout Experiment (TIBEX) performed at the Grimsel Test Site (GTS) aims to induce borehole failure in a controlled manner, using a borehole heater device by generating thermo-elastic stresses. This methodology mimics breakouts formation in deep wells that form when the rock is recovering its initial temperature after being cooled during the drilling process. The estimation of the needed hoop stress for inducing failure is a key parameter of this study.

Methods

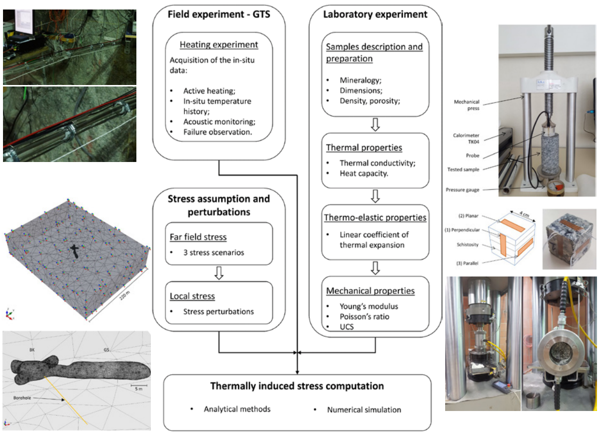

Figure 1: Workflow of the study: Field experiment at the GTS; Stress assumption and perturbations; Laboratory experiment; Thermally induced stress computation.

Theory

Thermo-elastic stress $S_{\Delta T}$ is an important component to assess stress condition and failure at the wall of deep geothermal wells. Thermo-elastic stresses can be approximated by using an analytical solution from Stephens and Voight [1]:

$$S_{\Delta T} = \frac{\alpha_0 E \Delta T}{1 - \nu} \quad \text{Eq. 1}$$

Superposing it to the stress concentration arising at wellbore wall $(r = a)$ using the Kirsch equation allows deriving the total hoop stress at the borehole wall:

$$\sigma_{\theta\theta} = \sigma_H + \sigma_h - 2(\sigma_H - \sigma_h)\cos 2\theta + \Delta P + S_{\Delta T} \quad \text{Eq. 2}$$

Depending on the authors, spalling effect is expected for a stress magnitude at the borehole wall $(\sigma_{\theta\theta})$ between 0.6 to 1 Uniaxial Compressive Strength (UCS) of the rock, although there is no general consensus on the actual wellbore wall strength.

Analytical computation of thermally induced stress

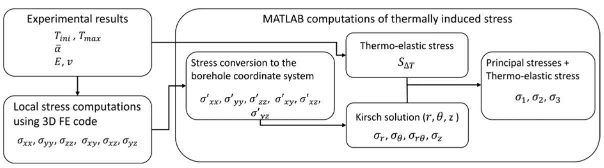

Figure 2: Method for analytical computation of thermally induced stress.

Results

Analytical Computation of Thermally Induced Stress

Stress along the borehole is computed using the analytical solution of Stephens and Voight [1] and the complete form of the Kirsch solution, for three far-field stress scenarios (Figure 3).

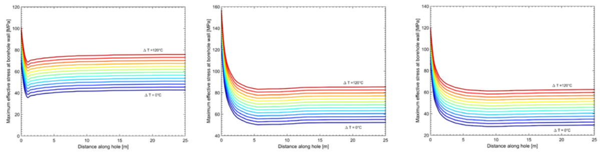

Figure 3: Analytical solution for thermally induced stress.

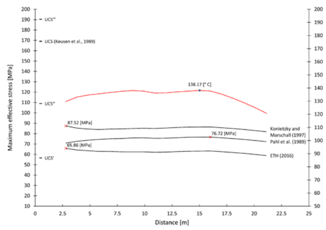

Using the temperature history from the in-situ TIBEX experiment, we computed the maximum effective principal stress acting on the borehole wall (Figure 4).

Figure 4: Maximum effective principal stress considering three stress scenarios ([2], [3], [4]), and compared to measured and estimated UCS.

Numerical simulation of thermo-elastic stresses

Using COMSOL Multiphysics 5.3, we simulated thermo-elastic stress in the surrounding rock of the 15 m depth borehole section (Figure 5).

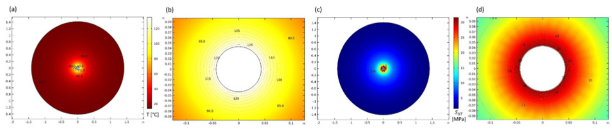

Figure 5: Numerical simulation of: (a), (b) temperature repartition; (c), (d) thermo-elastic stress

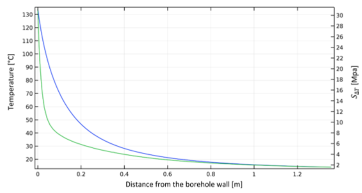

The simulation of the temperature and the induced thermo-elastic stress distribution in the surrounding rock is presented on Figure 6.

Figure 6: Numerical simulation of thermo-elastic stress (green curve) and temperature (blue curve) around the investigated borehole.

Conclusion

The experimental setup and the method used in this study proved their efficiency for heating a borehole of a ΔT of 120° C and reliably computing the induced thermo-elastic stress. The maximum effective principal stress at the borehole wall was estimated in a range between 60 and 80% of the UCS. However, no spalling was observed. This provides some constraints on the minimum wellbore wall strength. Future studies will be performed in higher stress conditions to generate failure.

References

[1] Stephens, G. & Voight, B. (1982). Hydraulic fracturing theory for conditions of thermal stress. International Journal of Rock Mechanics and Mining Sciences & Geomechanics Abstracts, 19(6), 279-284.
[2] Konietzky, H. & Marschall, P. (1997). Excavation Disturbed Zone around tunnels in fractured rocks-example from Grimsel Test Site. page 235-240, Rotterdam. Balkema.
[3] Pahl, A., Heusermann, S., Bräuer, V. & Glögger W. (1989). Grimsel test site: Rock Stresse investigations. Technical Report TR 88-39E, Nagra, Baden.
[4] Ziegler, M., Loew, S. & Amann, F. (2016). Near-surface rock stress orientations in alpine topography derived from exfoliation fracture surface markings and 3D numerical modelling. International Journal of Rock Mechanics and Mining Sciences, 85, 129–151. doi:10.1016/j.ijrmms.2016.03.009.

SCCER SoE
SWISS COMPETENCE CENTER for ENERGY RESEARCH
SUPPLY of ELECTRICITY

SCCER-SoE Annual Conference 2018

70 NRP Energy Turnaround
National Research Programme

Supported by:
Schweizerische Eidgenossenschaft
Confédération suisse
Confederazione Svizzera
Confederaziun svizra

Swiss Confederation

Innosuisse – Swiss Innovation Agency

Penetration depth of meteoric water and maximum temperatures in orogenic geothermal systems

Larryn W. Diamond, Christoph Wanner, H. Niklaus Waber
Rock–Water Interaction, Institute of Geological Sciences, University of Bern

Motivation

Orogenic belts without active igneous activity are recognized as plays for geothermal energy. In these systems, meteoric water circulation is typically expressed by thermal springs discharging at temperatures up to 70 °C from deep-reaching faults. The hydraulic gradients that drive circulation arise from the conjunction of high orographic precipitation, mountainous topography and permeable faults that link topographic highs with valley floors via the hot bedrock. Since the bedrock geotherm is the only source of heat for the circulating water, its maximum depth of penetration defines the maximum temperature attainable by surface springs and their upflow zones, thereby setting limits on their potential for geothermal energy exploitation. In the framework of the SCCER-SoE Task 1.1 we have performed geochemical modeling on chemically and isotopically well-characterized thermal waters currently discharging from the orogenic geothermal system at Grimsel Pass (Switzerland) to unravel the maximum penetration depth of meteoric water in such systems.

The Grimsel Pass geothermal system

- Discharge of warm springs with $T \leq 28$ °C into a gas tunnel beneath Grimsel Pass
- The springs occur where the tunnel intersects the WSW–ENE-striking Grimsel Breccia Fault (GBF), a major regional strike-slip shear zone
- Stable water-isotope analyses reveal a meteoric fluid origin
- Hydrothermal activity is also manifested by 3 million year old hydrothermal breccias formed ~2 km below the paleosurface
- Fluid inclusions in quartz and adularia indicate breccia formation at 165 °C (Hofmann et al., 2004)

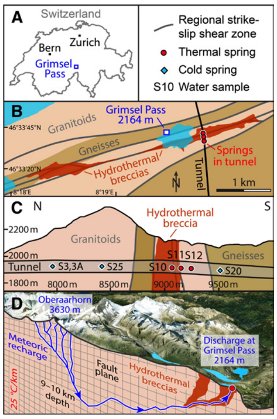

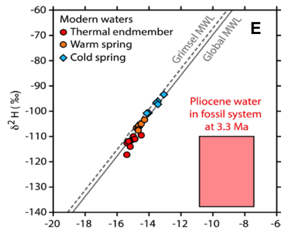

Fig. 1: (A) Location of Grimsel Pass. (B) Geological map with tunnel trace showing spatial coincidence between regional strike-slip faults, hydr. breccias and currently active warm springs. (C) Cross-section along the tunnel showing sampled springs. (D) Regional view to NNW showing conceptual present-day flow path of meteoric water along subvertical strike-slip fault. (E) Stable O–H isotopes in spring waters.

Approach

- Chemical and isotopic analyses of cold and warm springs
- Correction for admixture of modern surface water using ^{3}H, Na and Cl
- Numerical simulation (1D) of chemical evolution of thermal water as it rises and cools from its maximum penetration depth
- Assumption of chemical equilibrium between thermal water and granitic host rock at the lower model boundary (quartz + albite + muscovite + microcline)
- Dissolution reactions during upflow suppressed at T defined by Na/K ratio (= min-T_{eq})
- Precipitation reactions during upflow suppressed at T defined by silica geothermometer (T_{qtz}=174 °C), as this matches reconstructed SiO_2 conc. in warm springs
- Iterative determination of deep fluid temperature (min-T_{eq}) by comparing simulated with observed geothermal endmember composition at tunnel level

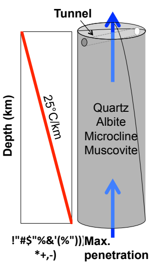

Fig. 2: Model setup

Reconstruction of the geothermal endmember water

- All warm springs show a detectable ^{3}H activity, despite the inferred residence time of 30 ka (Waber et al., 2017)
- Further, they show a strong linear correlation between Na and Cl
  - ➢ Represents a mixture of an old geothermal water with a modern cold water (Waber et al., 2017)
- Cold water fractions were reconstructed using coupled binary mixing models for Na, Cl and ^{3}H, while assuming that the thermal water is ^{3}H free (minimisation of uncertainty)
- Indicates cold water fractions of 50–70% in the various spring samples
  - ➢ Allows the composition of the geothermal endmember water to be determined at the tunnel level

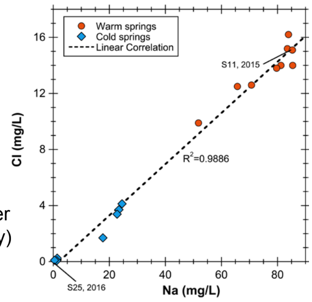

Fig. 3: Linear relationship between Na- and Cl-concentrations observed in warm and cold springs.

Results of geochemical modeling (TOUGHREACT V3)

- The Na/K ratio of the thermal water at depth is controlled by the following temperature-dependent equilibrium:
  Albite + K⁺ = Microcline + Na⁺
- Precipitation of small amounts of microcline and muscovite during upflow does not significantly change the Na/K ratio
- Setting min-T_{eq} to 214 °C explains the observed composition of the geothermal endmember water at the tunnel level
- As chemical equilibrium likely prevails along the hottest and deepest section of the flow path, the max. temperature is very probably 230–250 °C
- The local 25 °C/km geotherm is the only heat source. Attainment of 230–250 °C therefore requires a penetration depth of at least 9–10 km
- The Grimsel Pass system is unusually favorable for application of the Na–K solute geothermometer (cf. Giggenbach, 1998)
  - ➢ Similar penetration depths are possible at other orogenic geothermal systems worldwide

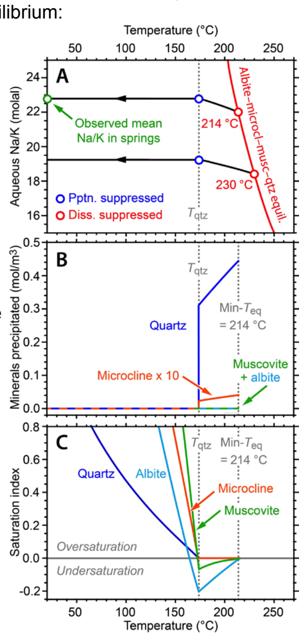

Fig. 4: Numerical simulation of the chemical evolution of the thermal water upon upflow and cooling. (A) The observed Na/K ratio of the thermal endmember water at its discharge site is reproduced if the minimum temperature of equilibrium between the water and its wall rock (min-T_{eq}) is set at 214 °C. (B) Amounts of minerals precipitated in a nominal 40 year period of upflow in mol per m³ of porous rock. (C) Saturation indices normalized to the amount of Si in each mineral.

Conclusions

- This study provides robust evidence that in the Grimsel Pass geothermal system, meteoric water has penetrated at least 9–10 km deep into the continental crust to attain 230–250 °C.
- Far more enthalpy may be accessible for exploitation around the upflow zones of orogenic geothermal systems than previously thought.!

References

Giggenbach, W.F. 1998. Geochimica et Cosmochimica Acta 52. 2749-2765. Hofmann, B. A. et al. 2004: Schweizerische Mineralogische und Petrographische Mitteilungen 84, 271-302. Waber, H.N. et al. 2017. Procedia Earth and Planetary Science 17. 774-777.

SCCER SoE
SWISS COMPETENCE CENTER for ENERGY RESEARCH
SUPPLY of ELECTRICITY

unine UNIVERSITÉ DE NEUCHÂTEL

SCCER-SoE Annual Conference 2018

swisstopo

Supported by:
Schweizerische Eidgenossenschaft
Confédération suisse
Confederazione Svizzera
Confederaziun svizra

Swiss Confederation

Innosuisse – Swiss Innovation Agency

How can the borehole three-dimensional displacement data help improving in situ stress estimation across a fault reactivated by fluid injections?

Maria Kakurina[1], Yves Guglielmi[2], Christophe Nussbaum[3] and Benoit Valley[1]

(1)University of Neuchâtel, CHYN, Neuchâtel, Switzerland, (2) Lawrence Berkeley National Laboratory, Berkeley, CA, United States, (3)Swisstopo, Wabern, Switzerland

Introduction

Standard in-situ stress measurement methods using fluid injection in deep boreholes are based on the analyses of pressure, flowrate and post-injection fracture mapping. Here we apply a new methodology to improve the estimation of the in-situ stress by adding the record of three-dimensional (3D) displacement in the pressured interval measured continuously during the injection. The direct measurement of displacements corresponding to slip on reactivated faults appear as a critical information to obtain the orientations and relative magnitudes of the principal stress components. Here we investigate and compare the data from two fault reactivation experiments conducted in carbonate rocks at the Rustrel Low Noise Underground Laboratory (LSBB URL), France, and in shale rocks at the Mont Terri Underground Laboratory, Switzerland. Both experiments consisted of fluid injections into the fault damages zone to reactivate the fault planes and trigger the slip, which will be used for solving the stress inverse problem.

Experimental and geological settings

The experiments protocol followed the step-rate injection method for fracture in-situ properties (SIMFIP) developed by Guglielmi et al. (2013). In comparison to standard double packer probes, the SIMFIP probe allows measuring the 3D displacement in the injection chamber together with the fluid pressure and flowrate. In both underground laboratories we performed pressure step-rate tests to activate a fault at different depths and different geological intervals (Figure 2). The experimental zone in carbonates includes the fractured damage zone of a natural fault. The experiment in Mont Terri has been conducted by injecting fluids in the upper, middle and lower parts of the main tectonic structure of the Opalinus Clay, called the Main Fault.

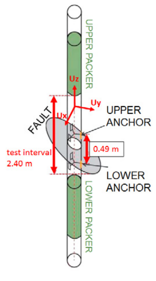

Figure 1. SIMFIP probe setup

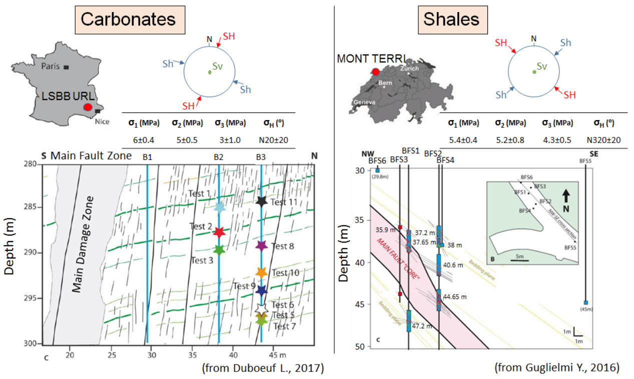

Figure 2. The experimental sites: left column – Rustrel LSBB URL, b) right column – Mont Terri URL. For each of the sites, there is an experimental location, far-field stress orientations and magnitudes, and cross sections showing the different testing intervals and simplified geology. Stars represent the 10 injection intervals.

Results

The maximum pressure in test 8 is 5.2 MPa, and in test 37.2 - 6.2 MPa. (Figure 3a). There is a linear flowrate-vs-pressure increase until 4.8 MPa in test 8 and 5.6 MPa in test 37.2 followed by a non-linear variation (Figure 3b). This pressure corresponds to the point when there is a significant increase in flowrate associated with a large displacement variation independently from pressure – Fault Opening Pressure (FOP). Below the FOP, the displacement linearly varies with pressure and correspond to the borehole expansion as well as to the poro-elastic response of the fracture. Above the FOP, the displacement shows independent non-linear response to pressure and a residual displacement is observed at the end of the test. We pick the displacement vectors when the pressure is "constant" in the interval. There are eight vectors in test 8 (carbonates) and seven vectors in test 37.2m (shales). The direction of the displacement vectors is given in Figure 4. The displacement vectors 1 to 4 in carbonates are aligned with the elastic response of the chamber that was observed below the FOP and orientated WNW.

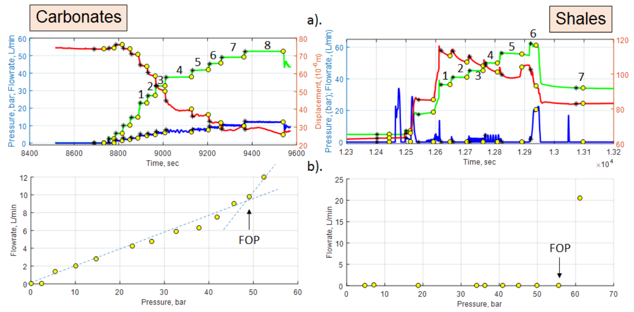

Figure 3. Protocol of the high-pressure step-rate test monitored during Test 8 in carbonates (left column) and Test 37.2 in shales (right column). (a) – Pressure (green), Flowrate (blue), Displacements (red) versus Time. Black asterisk and yellow circle are picked at each constant pressure step and correspond to the beginning end the end of the investigated (displacement) vector. (b) - Injected flowrate versus pressure (points correspond to the end on investigated vector.

At 4.8 MPa the displacement vector 7 shows a N310° dip direction and a 70° dip angle which are significantly different from the elastic response of the chamber. It is observed in Figure 4 that the vector 7 aligns with the fracture N135-72^0. It is interpreted as pure shear slip on that reactivated plane. The vectors 1 to 4 are located close to the pole of the fracture, interpreted as it is initial borehole opening. Vectors 5 and 6 correspond to the change between two directions and the vector 8 to the dilation of the activated plane. The displacements in test 37.2 m show more complex reorientations than in test 8. The displacement vectors mainly show almost normal opening of the bedding planes with a slight strike component. This is in a good accordance with the not-so-favorable orientation of the planes towards stress.

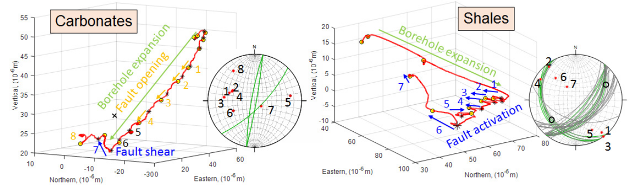

Figure 4. Orientations of the 3D displacement for carbonates (left) and for shales (right). Red asterisks correspond to the orientations of the displacement vector from the 3D plot. Black circles correspond to the potential fault slip under the far-field stress state. Green planes correspond to the planes located in the interval of the deformation unit of the SIMFIP probe.

Conclusions

In this study, we develop a protocol of how to estimate the in-site stress using the 3D displacement data obtained from the fault reactivation experiments. First, it was observed that the data obtained from shales is more complex. This may be caused by the difference in permeability and plasticity between carbonates and shales. However, it clearly appears that the activated fractures identified from the displacement measurements of both shales and carbonates match reasonably well with the stress tensors. Indeed, the fractures which are most favorably oriented towards the far-field stress are the ones which are identified from the analysis of the displacement vectors. Moreover, these vectors are useful in identifying the FOP, which can be consistent with the normal stress on the activated fracture. These data are then to be used to solve the reverse stress problem to estimate the in-situ stress. However, more work is required to estimate the range of the in-site stresses for all the tests, especially on the unicity of the solution using both the critical pressure values and the displacement vectors to estimate both the minimum and the maximum horizontal stress.

References

Duboeuf, L., De Barros, L., Cappa, F., Guglielmi, Y., Deschamps, A., & Seguy, S. (2017). Aseismic motions drive a sparse seismicity during fluid injections into a fractured zone in a carbonate reservoir. Journal of Geophysical Research: Solid Earth.

Guglielmi, Y. (2016). Mont Terri Project. Technical note 2015-60. Phase 21. In-situ clay faults slip hydromechanical characterizatiom (FS experiment), Mont Terri underground rock laboratory.

Guglielmi, Y., Cappa, F., Lançon, H., Janowczyk, J. B., Rutqvist, J., Tsang, C. F., & Wang, J. S. Y. (2013). ISRM suggested method for step-rate injection method for fracture in-situ properties (SIMFIP): Using a 3-components borehole deformation sensor. In The ISRM Suggested Methods for Rock Characterization, Testing and Monitoring: 2007-2014 (pp. 179-186). Springer International Publishing.

SCCER SoE
SWISS COMPETENCE CENTER for ENERGY RESEARCH
SUPPLY of ELECTRICITY

SCCER-SoE Annual Conference 2018

UNIL | Université de Lausanne

TU Delft
Delft University of Technology

Supported by:
Schweizerische Eidgenossenschaft
Confédération suisse
Confederazione Svizzera
Confederaziun svizra
Swiss Confederation
Innosuisse – Swiss Innovation Agency

Estimating fracture apertures and related parameters using tube-wave data

Jürg Hunziker, Andrew Greenwood, Shohei Minato, Eva Caspari and Klaus Holliger

Introduction

Fractures are only detected by televiewers if their aperture is above a resolution-dependent threshold. Furthermore, the inferred aperture is only representative within the immediate vicinity of the borehole. Tube-waves are interface waves, which are created at fractures and propagate along the borehole wall. Here, we use tube-waves to estimate the effective hydraulic fracture aperture, which is an average aperture related to the fluid content within the fracture. Furthermore, we also estimate the fracture compliance and the formation moduli.

Method

Full-waveform vertical seismic profiling (VSP) data serves as input for our stochastic inversion algorithm to infer the fracture parameters, the formation moduli, the standard deviation of the data error and the shape of the source-wavelet. As a forward solver we use the semi-analytical model derived by Minato and Ghose (2017). To sample the posterior distribution we use the DREAM(ZS) algorithm (ter Braak and Vrugt, 2008; Laloy and Vrugt, 2012), which is an efficient Markov chain Monte Carlo algorithm using differential evolution and parallel interacting chains to achieve faster convergence.

Results: Synthetic data with Gaussian noise

The test data were contaminated with Gaussian random noise. The depth of the fractures (10 and 50 m) and their inclination (10 and 45°) are assumed to be known from televiewer data. The receiver spacing is 0.1 m.

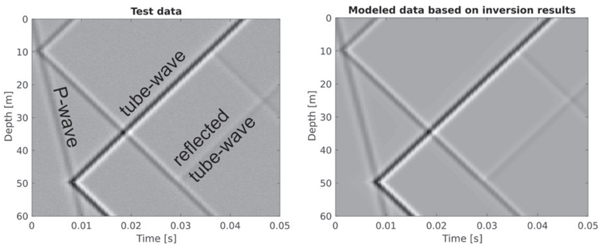

Results of the Markov chain Monte Carlo inversion. The weighted root mean square error and six unknowns estimated by the inversion are shown as functions of forward simulation steps. The estimates of the wavelet shown are samples taken from the end of the Markov chains.

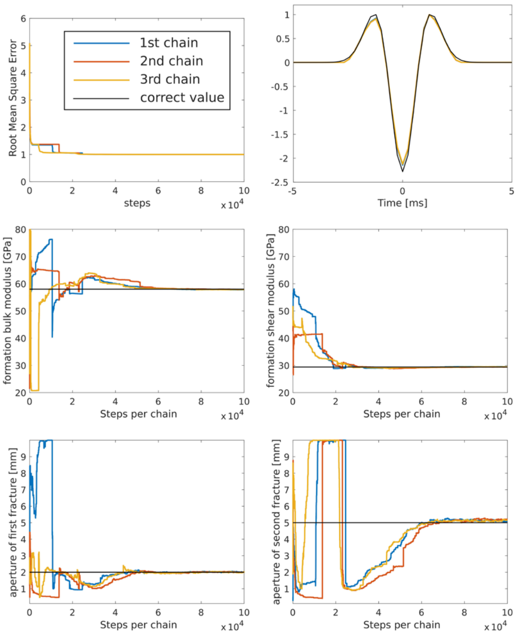

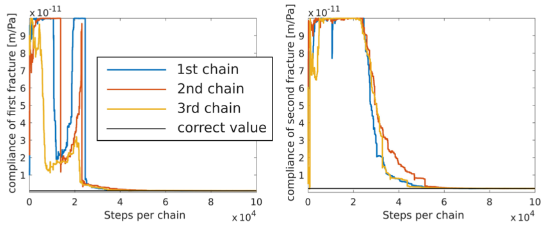

Results: Synthetic data with real noise

The synthetic test data were contaminated with real noise measured at the Grimsel Test Site in Switzerland. The fractures are located at 10 and 19 m depth. The receiver spacing has been increased from 0.1 m to 1 m.

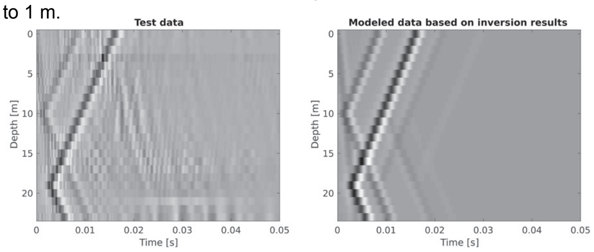

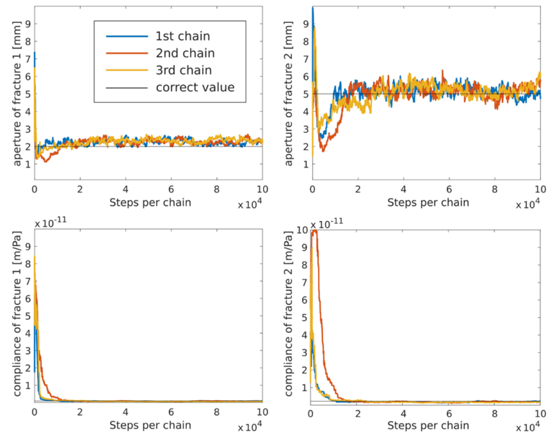

Conclusions

- The proposed tube-wave inversion approach allows to reliably estimate the fracture aperture, fracture compliance and the formation moduli.
- If the source wavelet is estimated incorrectly, the estimates of the remaining parameters are biased.

Outlook

- More reliable estimation of the source wavelet.
- Apply the algorithm on real data from the Grimsel Test Site in Switzerland.
- Longer Markov chains will allow to compute marginal posterior distributions of the unknowns.

References

- Laloy, E., & Vrugt, J. A., 2012: High-dimensional posterior exploration of hydrologic models using multiple-try DREAM(ZS) and high-performance computing, Water Resources Research, 48, WO1526.
- Minato, S. & Ghose, R., 2017: Low-frequency guided waves in a fluid-filled borehole: Simultaneous effects of generation and scattering due to multiple fractures, Journal of Applied Physics, 121, 104902.
- ter Braak, C. J. F., & Vrugt, J. A., 2008: Differential evolution Markov Chain with snooker updater and fewer chains, Statistics and Computing, 18, 435–446.

SCCER-SoE Annual Conference 2018

SCCER SoE
SWISS COMPETENCE CENTER for ENERGY RESEARCH
SUPPLY of ELECTRICITY

Supported by:
Schweizerische Eidgenossenschaft
Confédération suisse
Confederazione Svizzera
Confederaziun svizra
Swiss Confederation
Innosuisse – Swiss Innovation Agency
70 NRP Energy Turnaround
National Research Programme

Characterization of the fracture network in the damage zone of a shear fault with geophysical borehole methods

Eva Caspari[1], Ludovic Baron[1], Andrew Greenwood[1], Enea Toschini[1], Daniel Egli[2] and Klaus Holliger[1]
[1]University of Lausanne and [2]University of Bern

Introduction

Hydrothermally active shear zones in crystalline rocks are considered potential analogs for petrothermal reservoirs. The shear zone of interest in this study is the Grimsel breccia fault (GBF), a major WSW-ENE striking sub-vertical ductile shear zone in the Southwestern Aar Granite. The GBF has been exhumed from 3-4 km depth, is brittlely overprinted and exhibits fossil and active hydrothermal activity. A shallow borehole was drilled in 2015, which acutely intersects the main fault core and is situated in its damage zone. The focus is the characterization of the fracture network in the damage zone from geophysical borehole data. We employ geophysical logs to analyse fine-scale petrophysical variations, borehole radar (BHR) to image the fracture network and self-potential and fluid resistivity logs to examine the hydraulic system. To verify the observations we utilize the structural characterization of Egli et al. (2018).

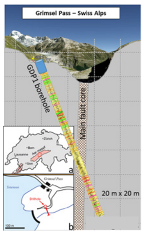

Petrophysical properties: Cluster analysis

A simple cluster analysis of some of the well logs (Figure 1) and a comparison (Figure 2) to the deformation data from the optical televiewer (OTV) shows that the response of the well logs and thus the variations in petrophysical properties are predominantly driven by the brittle deformation. As a result, the petrophysical properties can be categorized by four groups with varying intensity of brittle deformation.

Cluster groups:
1. Main fault core
2. Intensely fractured/Cataclastic
3. Highly fractured/ Large aperture fractures
4. Moderately fractured

Figure 1:

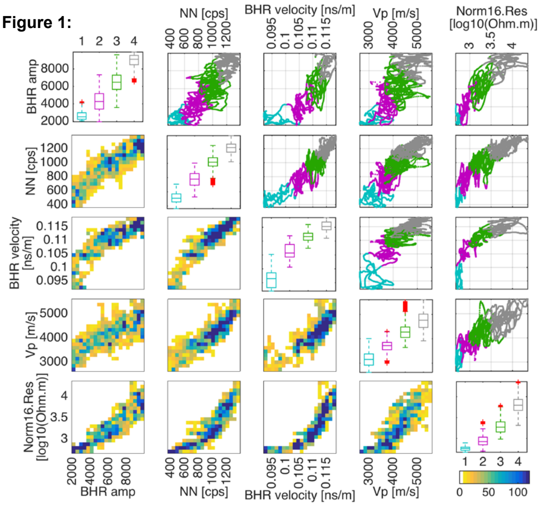

Figure 2:

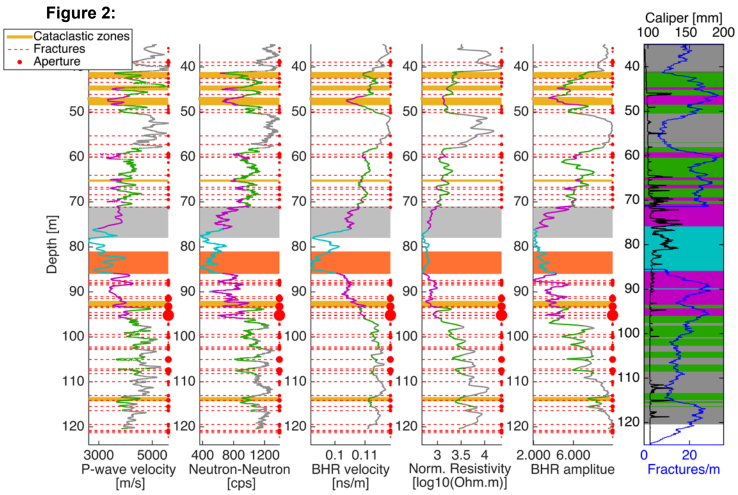

Fracture network: BHR and OTV

The migrated BHR image reveals a network of intersecting reflectors in the damage zone surrounding the main fault core (Figure 3a). A comparison of selected picked reflector dips with fractures dips from the OTV show a good agreement (Figure 3b) and thus, allows to link the reflections to fluid-filled fractures and cataclastic zones. The reflectors can be tracked a few meters into the formation in zones with low signal attenuation, which are indicated by the BHR first-cycle amplitude.

Figure 3:

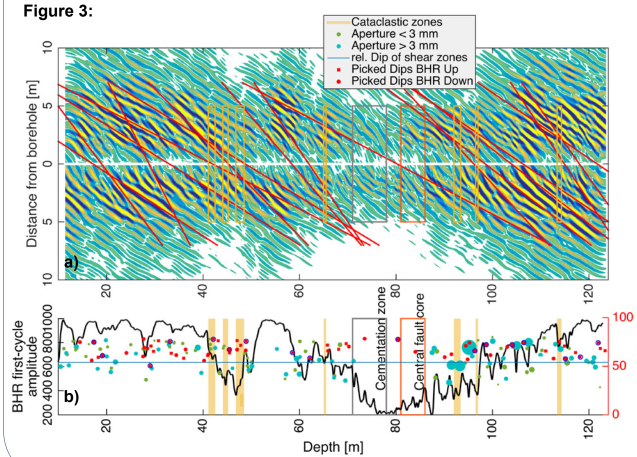

Hydraulic characteristics

The fracture network and cataclastic zones are the main flow pathways of the system. The self-potential data (Figure 4) contains an abundance of anomalies with varying magnitude, which can be linked to fractures and are likely to be of electrokinetic origin. As such they are indicative of zones of in- and out-flow into the borehole. Further, the fluid resistivity shows a distinctive layering. This may suggest the inflow of water from different sources and a compartmentalized system. The latter is supported by findings of Cheng et al. (2018) from pumping test. Their estimates of transmissivity are shown in Figure 4.

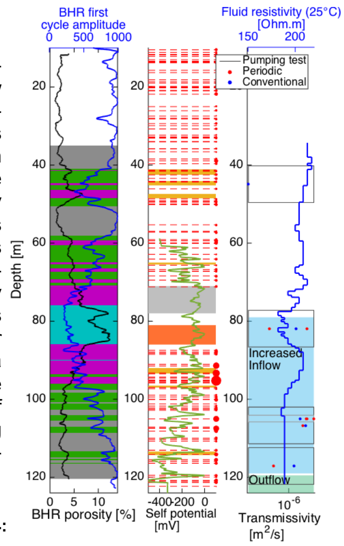

Figure 4:

References

Cheng, Y. and J. Renner (2018), Exploratory use of periodic pumping tests for hydraulic characterization of faults. *Geophysical Journal International* 212(1), 543-565.

Egli, D., Baumann, R., Küng, S., Berger, A., Baron, L. and M. Herwegh (2018), Structural characteristics, bulk porosity and evolution of an exhumed long-lived hydrothermal reservoir. *Tectonophysics* in submission

SCCER SoE
SWISS COMPETENCE CENTER for ENERGY RESEARCH
SUPPLY of ELECTRICITY

SCCER-SoE Annual Conference 2018

Supported by:
Schweizerische Eidgenossenschaft
Confédération suisse
Confederazione Svizzera
Confederaziun svizra
Swiss Confederation
Innosuisse – Swiss Innovation Agency

Attenuation and velocity anisotropy of stochastic fracture networks

Eva Caspari[1], Jürg Hunziker[1], Marco Favino[2], J. Germàn Rubino[3] and Klaus Holliger[1]
[1]University of Lausanne, [2]Universita della Svizzera italiana
and [3]CONICET, Centro Atómico Bariloche - CNEA, Argentina

Summary

Fracture networks tend to have preferential orientations, which in turn translate into anisotropy of the seismic velocity and attenuation. An attenuation mechanism of interest is fluid pressure diffusion due to its potential sensitivity to fracture network characteristics. There are two manifestations of the mechanism: fracture-to-background wave induced fluid flow (FB-WIFF) and fracture-to-fracture wave induced flow (FF-WIFF). In this study, we use a quasi-static poroelastic numerical upscaling procedure (Rubino et al. 2016, Favino et al. 2018) to model the aforementioned mechanism for anisotropic stochastic fracture networks with varying length distributions and fracture densities. The aim is to systematically analyse the dependence of the resulting attenuation and velocity anisotropy with regard to these network characteristics. Here we present preliminary results.

References

M. Favino, J. Hunziker, E. Caspari, B. Quintal, K. Holliger, R. Krause (2018), Fully-automated adaptive mesh refinement for the simulation of fluid pressure diffusion in strongly heterogeneous media, *submitted to Journal of Computational Physics.*

J. G. Rubino, E. Caspari, T. M. Müller, M. Milani, N. D. Barbosa, K. Holliger (2016), Numerical upscaling in 2-D heterogeneous poroelastic rocks: Anisotropic attenuation and dispersion of seismic waves, *Journal of Geophysical Research: Solid Earth*, 121, 6698-6721.

Anisotropic fracture networks

The fracture dip is limited to angles between 30° and 150°, where 0° denotes a vertical fracture and 90° a horizontal one. The characteristic exponent *a* defines the steepness of the distribution and *d* is the area covered by fractures.

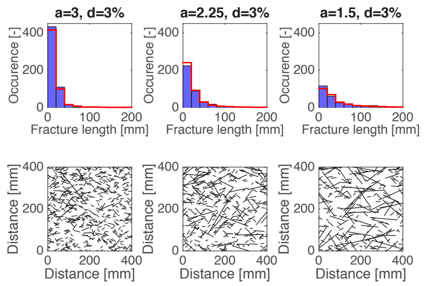

Network parameters	
Exponent *a*	1.5 -3
Length [mm]	10, 200
Fracture area *d* [%]	1.5 – 3.25
Aperture [mm]	0.5
Simulations per set	25

Velocity and attenuation as function of angle and frequency (a = 1.5)

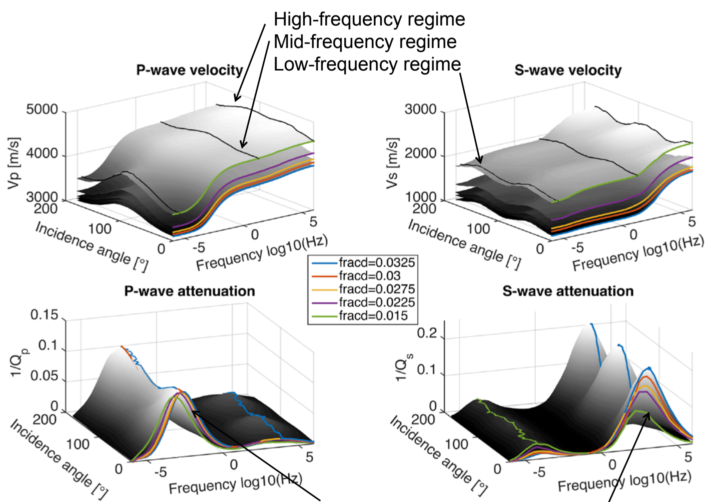

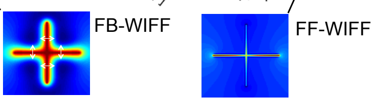

Figure 1: Each surface plot corresponds to the median of 25 realizations of the stochastic fracture networks.

Attenuation anisotropy

For P-waves, the attenuation anisotropy rotates by 45° between FF-WIFF and FB-WIFF. This is not the case for S-waves. In general, the attenuation increases with fracture area *d* and the exponent *a*. An exception is FF-WIFF for S-waves.

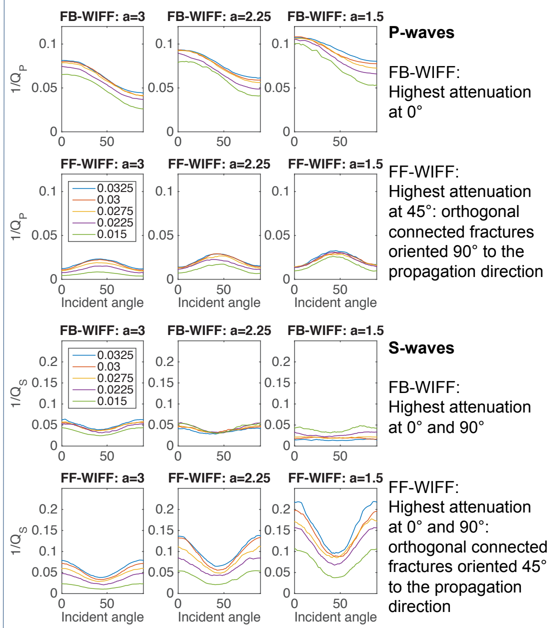

Figure 2: Variation of attenuation with incidence angle at the peak frequencies of FB-WIFF and FF-WIFF.

Velocity anisotropy

Overall, the velocity anisotropy is larger for P- than S-waves. For P-waves, the anisotropy is highest in the low-frequency regime and, in general, decreases with a decrease in the exponent *a*. Contrarily, for S-waves, the anisotropy tends to be higher in the high-frequency regime and increases with a decrease in the exponent *a*.

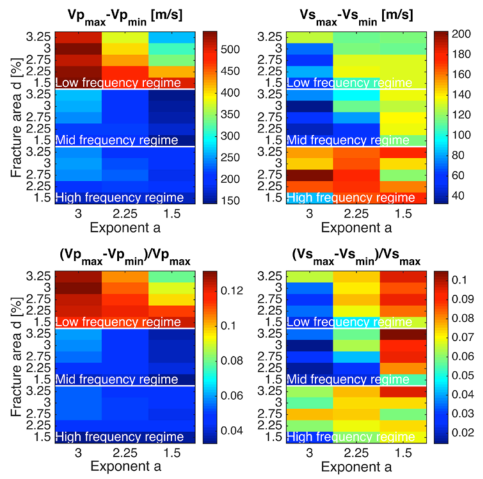

Figure 3: Maximum absolute and relative angle-dependent velocity change for three characteristic frequency regimes.

SCCER SoE
SWISS COMPETENCE CENTER for ENERGY RESEARCH
SUPPLY of ELECTRICITY

SCCER-SoE Annual Conference 2018

Supported by:
Schweizerische Eidgenossenschaft
Confédération suisse
Confederazione Svizzera
Confederaziun svizra
Swiss Confederation
Innosuisse – Swiss Innovation Agency

Seismic attenuation and P-wave modulus dispersion in poroelastic media with fractures of variable aperture distributions

Simón Lissa[1], Nicolás D. Barbosa[1], J. Germán Rubino[2], & Beatriz Quintal[1]

1 Institute of Earth Sciences, University of Lausanne, Switzerland.
2 CONICET, Centro Atómico Bariloche - Comisión Nacional de Energía Atómica, Argentina.

Introduction

Fractures in rocks occur in a wide range of scales and their identification and characterisation are important for several areas such as oil and gas exploration and extraction, production of geothermal energy, nuclear waste disposal, civil engineering works, among others. Given that seismic waves properties are significantly affected by the presence of fractures, seismic methods are a valuable tool for characterising them. In particular, when a fluid-saturated fractured rock is compressed by a propagating wave, a pressure gradient is generated due to the compressibility contrast between the fracture and the embedding background. Consequently, energy dissipation occurs during the corresponding fluid pressure equilibration process. This mechanism can be an important cause of seismic wave attenuation and stiffness modulus dispersion.
In this work we numerically quantify the effects of contact areas on seismic wave attenuation and P-wave modulus dispersion using 3D models containing a horizontal fracture.

Example of fractured rock

Methodology

- Biot's (1941) equations in the **u**-p formulation.
- Solved using finite element method.
- Relaxation test normal to the fracture (undrained conditions).
- Water saturated.

- Material properties:

	Background and contact areas	Open fracture
Grain bulk modulus [GPa]	K_s=37	K_s=37
Grain density [g/cm^3]	ρ_s=2.65	ρ_s=2.65
Porosity	ϕ_B=0.1	ϕ_{fr}=0.9
Permeability [mD]	κ_B=2.37	κ_{fr}=10^5
Dry rock bulk modulus [GPa]	K_m=26	K_m=0.02
Dry rock shear modulus [GPa]	μ_m=30	μ_m=0.01
Fluid bulk modulus [GPa]	K_w=2.25	K_w=2.25
Fluid density [g/cm^3]	ρ_w=1.09	ρ_w=1.09
Fluid viscosity [P]	η_w=0.01	η_w=0.01

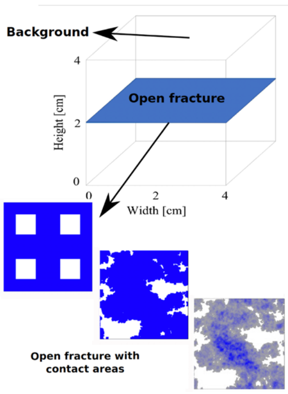

Effects of contact areas

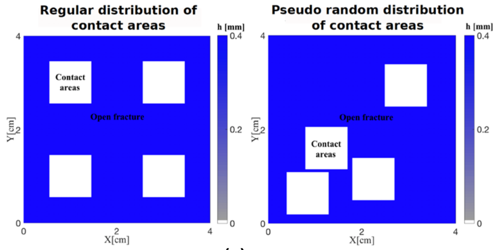

(a)
White: contact areas Blue: open fracture
Open fracture constant aperture = 0.4 mm.
Individual contact area size = 0.9 x 0.9 cm.
Contact area density = 20%.

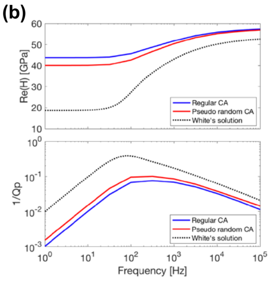

(b)
P-wave modulus (top) and attenuation (bottom) normal to the fractures as functions of frequency.

Regular distribution → - Attenuation
- Fracture excess compliance

Pseudo random distribution → + Attenuation
+Fracture excess compliance

Realistic aperture distributions

(a)
Fracture models with variable aperture. All models have a mean aperture of 0.4 mm.

(b)
Fracture models with binary aperture distribution. The aperture in the open fracture zone is set to the mean aperture.

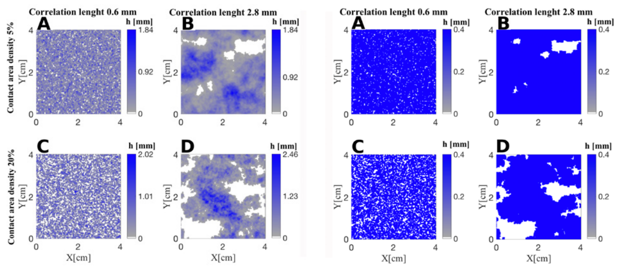

(c)
P-wave modulus and attenuation normal to the fractures as functions of frequency. Solid lines corresponds to fractures with variable aperture (Fig. 4a) while dashed lines correspond to fractures with binary aperture (Fig. 4b).

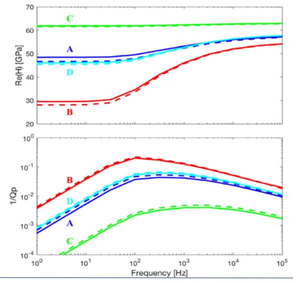

Comparison between realistic and simplified fracture models

P-wave modulus and attenuation normal to the fractures as functions of frequency. Solid lines correspond to models with variable aperture distributions (Fig. 4a). Dashed lines correspond to models with open fracture zones with constant aperture and without contact areas but using equivalent fracture bulk and shear modulus (which effectively incorporate the effect of contact areas) and equivalent porosity and aperture.

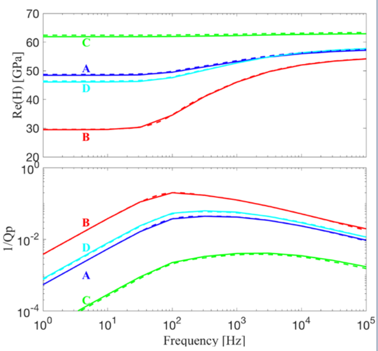

Conclusions

1. For a given contact area density, fractures with correlated distributions of contact areas exhibit higher P-wave modulus dispersion and seismic attenuation. Although the effects of distribution of contact areas is maximal at the low frequency limit, these distributions also play an important role in the effective compliance of the rock at the high frequency limit.

2. The seismic response of a fracture with realistic aperture distributions can be approximated by a thin layer with constant thickness, provided that appropriate equivalent poroelastic properties are employed.

Acknowledgments

This work has been supported by a grant from the Swiss National Science Foundation.

SCCER SoE
SWISS COMPETENCE CENTER for ENERGY RESEARCH
SUPPLY of ELECTRICITY

unine UNIVERSITÉ DE NEUCHÂTEL
CHYN Centre d'hydrogéologie et de géothermie
UNIVERSITÉ DE GENÈVE FACULTÉ DES SCIENCES Département des sciences de la Terre

SCCER-SoE Annual Conference 2018

GEOTHEST - Building an INTERREG project France-Switzerland on innovation in geophysical exploration for geothermal development in sedimentary basins.

Supported by:
Schweizerische Eidgenossenschaft
Confédération suisse
Confederazione Svizzera
Confederaziun svizra
Swiss Confederation
Innosuisse – Swiss Innovation Agency
UNIVERSITÉ SAVOIE MONT BLANC

Mauri G.(1), Got J-L.(2), Lupi M.(3), Trouver E.(2), Miller S.A.(4)

(1) previously Centre d'hydrogéologie et de Géothermie (CHYN), Université de Neuchâtel (UNINE), Neuchâtel, Switzerland (guillaume.mauri@unine.ch , g.mauri10@bluewin.ch)

(2) Université Savoie Mont-Blanc, Chambéry, France. (Jean-Luc.Got@univ-smb.fr, Emmanuel.Trouve@univ-smb.fr)

(3) Sciences de la Terre et de l'environnement, Université de Genève, Genève, Switzerland. (Matteo.Lupi@unige.ch)

(4) Centre d'hydrogéologie et de Géothermie (CHYN), Université de Neuchâtel (UNINE), Neuchâtel, Switzerland. (stephen.miller@unine.ch)

Context

In urban and peri-urban regions, such as Switzerland and France, the first stage of a geothermal study relies on active seismic acquisition methods (2D or 3D), which are costly and often logistically complex. Seismic data provide valuable information on contrasts of impedances between geological formations. However, geothermal reservoirs can either extend throughout several geological units or be confined within one lithology. Hence, it is key to first constrain the extent of the geothermal reservoir.

For hydrothermal reservoirs new and innovative electrical methods, such as Deep Electrical Resistivity Tomography (DERT), are cost-effective and logistically easy to handle (from topography surface to 1km depth).

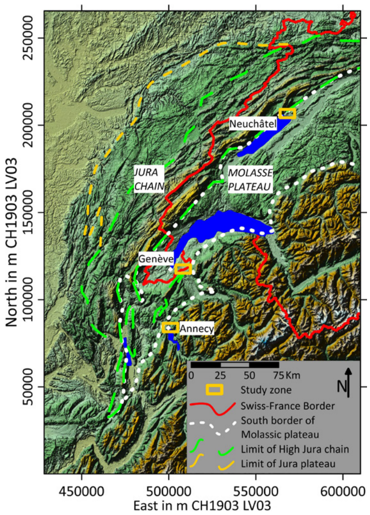

For reservoirs at larger depths (i.e. below 1 km) magnetotelluric methods (MT) are a viable solution. However, in urban areas the electrogmagnetic noise is often too strong, and MT cannot properly locate the reservoir.

Figure 01: Geographical context of western Switzerland and along the French border. Both Jura mountain range and Molasse plateau are extending from Switzerland to France. The city names locate the study area for GEOTHEST project.

France-Swiss Collaborations

GEOTHEST is an INTERREG project, which is currently in preparation.

It groups two Swiss universities with a French university.

- University of Neuchâtel, Center for Hydrogeology and Geothermics,
- University of Geneva, Earth and environmental Sciences,
- University Savoie Mont Blanc.

It is supported by the:

- Canton of Neuchâtel,
- Industrial Services of Geneva (canton of Geneva)
- Foundation of University Savoie Mont Blanc,
- Communities of Pays de Gex, Genevois, Annecy, Aix-les-Bains, Chambéry.

The Pre-project has been accepted by the INTERREG OFFICE.

Presentation of INTERREG V France-Swiss

INTERREG V France-Swiss is a program of inter-region cooperation founded by the EU and in which Switzerland is a partner.

INTERREG V France-Swiss are bringing together resources, structures from the different region and supporting innovative projects, particularly in the energy field.

Objectives of the Project

The GEOTHEST project aims to develop:

- 1) develop a new methodology for both acquisition and data analyses for MT to overcome electromagnetic distortion from human activity,
- 2) apply DERT surveys to better characterize shallower reservoir,
- 3) build on and improve on existing models to more accurately characterize geothermal reservoirs,
- 4) for the site of Annecy in France, the project also includes a hydrogeological model of the area. Such hydrogeological models for the two sites in Switzerland already exist.

The project will be submitted later this fall and we are searching for industrial partners

Concept

The project implements the innovative method and applies it to investigate geothermal reservoirs at 3 study sites in France and in Switzerland.

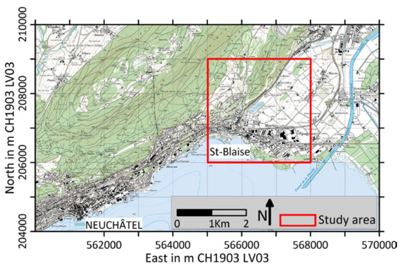

Figure 02: Localisation of the study area near Neuchâtel (CH).

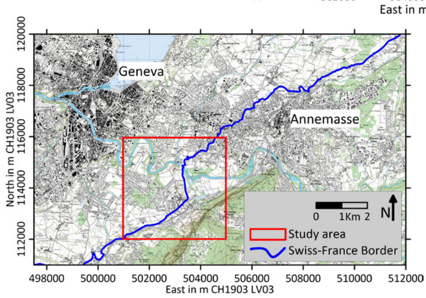

Figure 03: Localisation of the study area in the transborder zone, near Annemasse (France) and Geneva (CH).

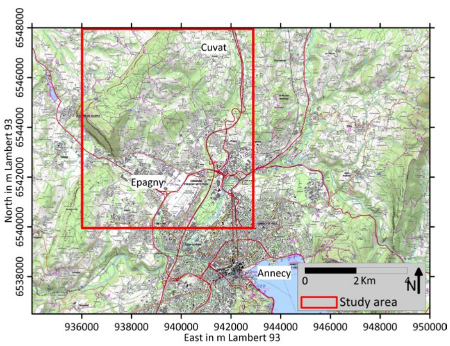

Figure 04: Localisation of the study area near Annecy (France).

Acknowledgement

We are thankful to the representative of University Savoie Mont Blanc, University of Neuchâtel, & University of Geneva for their support. We are grateful to Canton of Neuchâtel, Industrial Services of Geneva, Fondation of University Savoie Mont Blanc, Communities of Pays de Gex, Genevois, Annecy, Aix-les-Bains, Chambéry for their support and their financial contribution.

SCCER-SoE Annual Conference 2018

SCCER SoE
SWISS COMPETENCE CENTER for ENERGY RESEARCH
SUPPLY of ELECTRICITY

UNIVERSITÄT BERN

Supported by:
Schweizerische Eidgenossenschaft
Confédération suisse
Confederazione Svizzera
Confederaziun svizra
Swiss Confederation
Innosuisse – Swiss Innovation Agency

Reactive transport models of the orogenic hydrothermal system at Grimsel Pass, Switzerland

Peter Alt-Epping, Larryn W. Diamond & Christoph Wanner
Rock-Water Interaction, Institute of Geological Sciences, University of Bern

1) Introduction

Thermal waters at temperatures in the range of 17 – 28 °C discharge into a tunnel underneath Grimsel Pass in the Central Alps. The thermal springs are located at an elevation of about 1900 m.a.s.l.. Discharge occurs at low rates (≤ 10 L/min) along the Grimsel Breccia Fault (GBF), which is exposed some 100 m within the tunnel. Geochemical evidence suggests that the water is a mixture of old geothermal water and younger cold water components having residence times of at least 30 ky and about 7 years, respectively. Both components are meteoric in origin (Waber et al., 2017). Reconstruction of the temperature of the geothermal component alone yields a discharge temperature of ~50 °C.

We use the high performance reactive-transport code PFLOTRAN (*www.pflotran.org*) to model the hydrothermal system in its entirety (i.e. the recharge zone, the reaction zone down to a depth of 10 km and the upflow and discharge zones below Grimsel Pass) and to integrate geological, hydrological, thermal and geochemical observations. We perform simulations that obey the chemical, hydraulic and thermal constraints of the discharging water and the mineralogy of a spatially coincident fossil (3 Ma) upflow zone cemented by quartz and adularia (Hofmann et al., 2004; Belgrano et al., 2016), to explore feasible permeability distributions and flow patterns in the deep fault zone. One of the issues to be resolved is how water recharging the fault system at high altitude can penetrate the rock to a depth of about 10 km and attain the maximum system temperature of about 250 °C as estimated from solute geothermometry.

2) Constructing a regional scale model of the Grimsel system

The main driving force for fluid flow in the Grimsel system are gradients in elevation head due to topography of the region. Constructing a 3D model domain that incorporates the regional topography as upper boundary involved the following steps:

Produce a grid of the topographic surface (easting/northing and elevation)

↓

Create a mesh of the surface grid through Delaunay triangulation

↓

Use a mesh generator to add 3rd (depth) dimension and geological structures

↓

Convert 3D mesh into PFLOTRAN format, initialize P and T fields

3) Numerical model

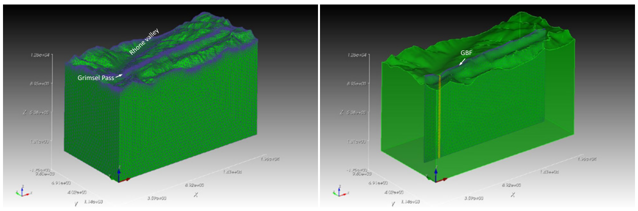

Model dimensions and grid. The GBF (right) is modelled as vertical fault plane extending to a depth of about 10 km. It constitutes a zone of higher permeability. The upflow zone below the Grimsel thermal springs is shown in yellow. It has a permeability of $1{\times}10^{-13}$ m^2. The system is heated from below at a constant rate of 0.0705 W/m^2 consistent with background heat flow values. Quartz is the only reacting mineral in the model.

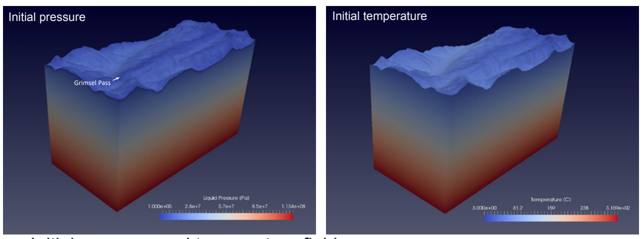

Initial pressure and temperature fields

4) Model results

Fluid circulation is driven by meteoric recharge into the GBF at high elevation and focussed discharge of hydrothermal fluid at lower elevation at Grimsel Pass. The permeability contrast between the GBF and the surrounding rock allows the fluid to infiltrate the rock to depths of 10 km (or more). Through water-rock interaction along its pathway the fluid obtains its thermal and chemical fingerprint. The breakthrough of a tracer injected with the infiltrating fluid is used to illustrate the flow pattern and calibrate fluid residence times and fault permeabilities.

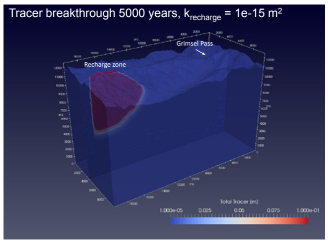

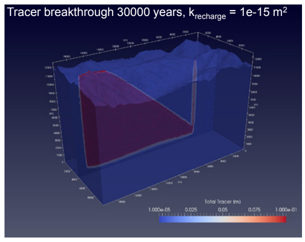

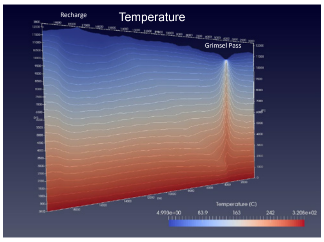

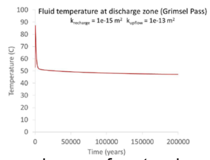

Diffuse recharge of meteoric water leads to a weak depression of isotherms, whereas focussed upflow induces a distinct thermal anomaly.

Breccia with silicified matrix at Grimsel Pass
Belgrano et al, 2016

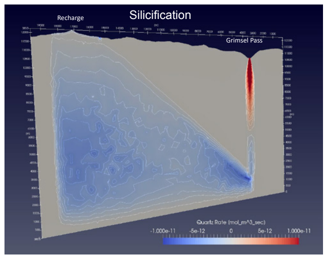

Silicification is ubiquitous in the GBF at Grimsel Pass within the paleo-upflow zone (left). The model predicts large quantities of quartz to precipitate within the upper part of the upflow zone (i.e. < 6 km depth) where the fluid undergoes cooling (right).

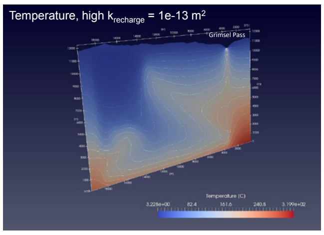

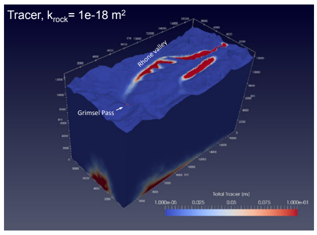

Model variants. A uniform high permeability throughout the recharge zone leads to convective circulation within the zone (left). A high permeability of the rock increases discharge into the surrounding valleys (right).

5) Conclusions

We established a workflow from a GIS-based surface grid to a regional-scale 3D PFLOTRAN reactive transport model. Simulations show that fluid recharge to a depth of 10 km requires focussed flow along (one or several) higher permeability pathways.

REFERENCES:
Belgrano, T. M., Herwegh, M. & Berger A. 2016: Inherited structural controls on fault geomttry, architectureand hydrothermal activity: an example from Grimsel Pass, Switzerland, Swiss J Geosci, 109, 345-364.
Hofmann, B. A., Helfer, M., Diamond, L. W., Villa, I., Frei, R., and Eikenberg, J., 2004, Topography-driven hydrothermal breccia mineralization of Pliocene age at Grimsel Pass, Aar massif, Central Swiss Alps: Schweizerische Mineralogische und Petrographische Mitteilungen, v. 84, no. 3, p. 271–302
Waber, H.N., Schneeberger, R., Mäder, U.K., Wanner, C. 2017: Constraints on evolution and residence time of geothermal water in granitic rock at Grimsel (Switzerland). 15th Water-Rock Interaction Syposium, WRI-15, Procedia Earth and Planetary Science 17, 774-777.

Contact: alt-epping@geo.unibe.ch

SCCER SoE
SWISS COMPETENCE CENTER for ENERGY RESEARCH
SUPPLY of ELECTRICITY

SCCER-SoE Annual Conference 2018

In cooperation with the CTI
Energy
Swiss Competence Centers for Energy Research
Schweizerische Eidgenossenschaft
Confédération suisse
Confederazione Svizzera
Confederaziun svizra
Swiss Confederation
Commission for Technology and Innovation CTI

Compilation of data relevant for geothermal exploration – a first step towards a Geothermal Play Fairway Analysis of the Rhône Valley

D.B. van den Heuvel, S. Mock, D. Egli, L.W. Diamond, M. Herwegh (Institute of Geological Sciences, University of Bern)

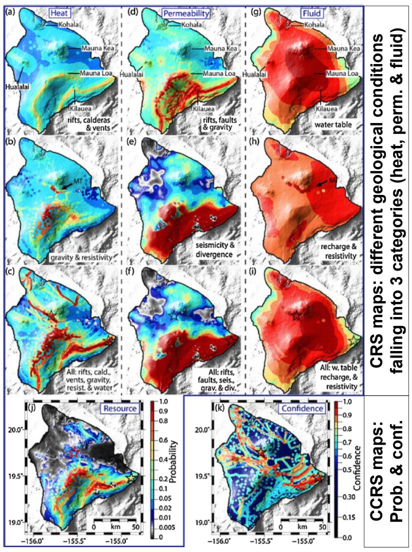

Play Fairway Analysis Hawaii Island
From Ito et al. (2017)

1. What is a Geothermal Play Fairway Analysis (PFA)?

→ Tool adapted from hydrocarbon exploration industry: Spatial correlation of data relevant for geothermal systems

→ Step by step:

① Compile existing data

② Examine, integrate and interpret data (→ create GIS maps)

③ Construct probability maps for each geologic condition (common risk segment CRS map)

④ Integrate individual maps to a composite common risk segment (CCRS) map

⇒ **Favourability map highlighting areas with high chance of exploration success**

2. Geothermal activity in the Rhône Valley

Most active geothermal domain in Switzerland

→ Many known occurrences of thermal water

→ Most not (yet) exploited (few used for district heating)

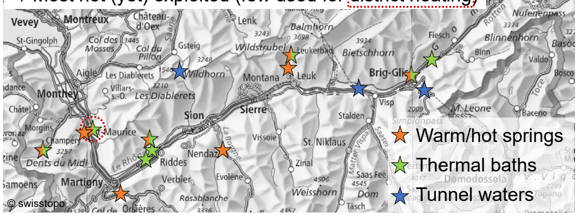

Why?

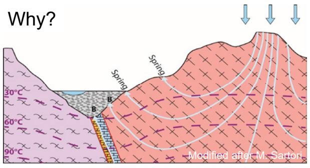

→ Fluid circulation is gravity driven (up to 10 km depth, i.e. up to 250 °C[1])

→ Heat source = background geothermal gradient (~25 °C / km)

More thermal water discharge areas expected than the ones currently known

→ Obscured by the thick Quaternary sediments (up to 900 m)[2] and mixing with GW (no surface expression = "blind" system **B**)

→ **Perform a geothermal PFA to find such blind systems**

3. Geothermal PFA Rhône Valley – data compilation

Data sources:

→ Online mapping platform of Switzerland

→ Geologic and Tectonic maps of Switzerland

→ Database on Swiss geothermal fluids[3]

→ Database on geothermal boreholes [4-7]

→ Evaluation geothermal potential of VS[8] & VD[9]

→ Nationwide & regional geophysical surveys[10-14]

→ Journal articles, BFE reports etc.

Categorise and discuss data available :

Background

- Basics: *Infrastructure*; *Well & spring loc.*; *Protected areas*
- Geology: *Surface geology*; *Thickness of quat. sediments*
- Seismicity: *Seismic hazard*; *Historical earthquakes*
- GW & river hydrogeol.: *Chemical composition*; *Isotopic composition*; *Temperatures*; *Water level*; *Flow rates*

Heat source

- Geophys.: *Gravimetry*; *Geomagnetics*; *Magnetotellurics*
- Fluid: *Chemical composition*; *Isotopic composition*
- Temp.: *Direct measurement*; *Geothermometry*
- *Place names related to thermal water occurrence*

Permeability

- *Tectonic & structural regime/setting*
- *Regional stress field*
- *Shear & dilat. strain*
- Fault geom.: *Age*; *Length*; *Displacement*; *Slip & dilat. tendency*; *Interfault geometry*

Problems:

- Well data of thermal baths and NEAT confidential
- Age of data: Mostly data collected during the 80s and 90s → Reliability of decades old data?
- Mostly point data at locations with known thermal occurrence; few regional studies or relevant data away from known occurrences

4. How to proceed with the geothermal PFA?

By the end of 2018:

→ Finish creating individual GIS layers for each *topic*

→ Combine the GIS layers of each topic within a subcategory

→ Write a report discussing the data available and its quality

→ Identify areas with a lack of data and the datasets which would benefit most from expanding
Suggestion for future sampling campaigns

→ Coordinate the publication of the GIS maps with Swisstopo

In the long run:

→ Extrapolate point data (e.g. by inverse distance weighting (IDW) or kriging) to create a CRS map for each subcategory

→ Combine the CRS maps of the subcategories to two CCRS maps (**heat source** and **permeability**) by a multi-criteria-decision making (MCDM) process

→ Combine these two CCRS maps to an overall favourability map
Permeability < 50% as a site with little or no permeability could potentially be developed as an EGS system

→ Add layers from the **background** maps such as «protected areas» and «seismicity» to exclude sensitive areas

→ Identify most promising location for a detailed site investigation

In collaboration with:
Schweizerische Eidgenossenschaft
Confédération suisse
Confederazione Svizzera
Confederaziun svizra
Bundesamt für Landestopografie swisstopo
Office fédéral de topographie swisstopo
Ufficio federale di topografia swisstopo
Uffizi federal da topografia swisstopo

Funded by:
Schweizerische Eidgenossenschaft
Confédération suisse
Confederazione Svizzera
Confederaziun svizra
Bundesamt für Energie BFE
Swiss Federal Office of Energy SFOE

References:
[1] Wanner et al., *Geol.*, in revision. [2] Klingele, *SGPK*, 2012. [3] Sonney & Vuataz, *Geoth.* 2008. [4] Schärli & Kohl, *SGPK*, 2002. [5] Boulicault et al., Proceedings SGM 2017. [6] Géocadastre VS geocadast.crealp.ch. [7] Géocadastre VD www.geo.vd.ch/theme/localisation_thm [8] Vuataz et al. *Bull. Cent. Hydrogeol. Univ. Neuchâtel*, 1993. [9] Wilhem et al., *BFE Report*, 2003. [10] Bodmer & Rybach, *SGPK*, 1982. [11] Klingele, *SGPK*, 1982. [12] Medici & Rybach, *SGPK*, 1995. [13] Schnegg, *SGPK*, 1998. [14] Olivier et al., *SGPK*, 2010.

SCCER SoE
SWISS COMPETENCE CENTER for ENERGY RESEARCH
SUPPLY of ELECTRICITY

SCCER-SoE Annual Conference 2018

Supported by:
Schweizerische Eidgenossenschaft
Confédération suisse
Confederazione Svizzera
Confederaziun svizra
Swiss Confederation
Innosuisse – Swiss Innovation Agency

In-situ characterization of fluid flow in an EGS-analog reservoir

Brixel B. [1], *Jalali M.* [2], *Klepikova M.* [1], *Roques C.* [1], *Löw S.* [1]

[1] *Department of Earth Sciences, ETH Zürich, Switzerland*
[2] *Chair of Engineering Geology and Hydrogeology, RWTH Aachen, Germany*

Motivation, Goals & Objectives

Better understanding how heterogeneity impacts fluid flow and pore pressure diffusion in geological media *in-situ* is paramount for many disciplines in earth sciences as well as for industries relying on natural resources, including deep geothermal energy (DGE) applications - as is planned as part of the **Swiss Energy Strategy 2050**.

To this end, the goals of our study are to:

- Map out the **3-D permeability structure** of a fault zone (at borehole scale);
- Determine the **connectivity structure** of permeable domains and characterize **diffusion processes** therein;
- Identify the **backbone** of the fracture network amenable to flow, solute and heat transport.

Data used in this study were collected as part of the ISC experiment completed at the Grimsel Test Site, Switzerland (see Figure 1)

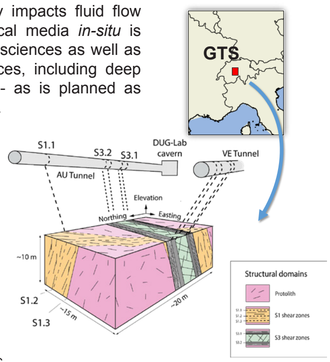

Fig. 1: Site location and geology

How «linear» is diffusion?

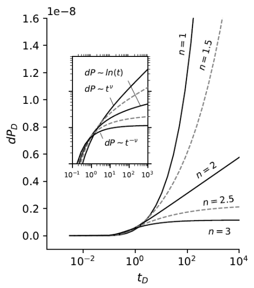

Fig. 2: Solution to Barker's model

Generalized radial flow (GRF) solution to a constant rate test, Barker [1988] :

$$dP(r,t) = \frac{Qr^{2-n}}{4\pi^{n/2}T}\Gamma\left(\frac{n}{2}-1, \frac{Sr^2}{4Tt}\right)$$

(projection of surfaces on a hypersphere)

$$\alpha_n = \frac{2\pi^{\frac{n}{2}}}{\Gamma(\frac{n}{2})}$$

Methods & Datasets

Data acquisition was carried out following standard hydrogeological field methods including single and cross-hole packer testing, the purpose of which is to induce a perturbation in the natural head field.

- Pressure pulse tests were used to compute discrete (i.e. local) Transmissivity (T) estimates, using Neuzil's method (Neuzil, 1982). These estimates were then used as a proxy for the permeability (k) structure.
- Constant rate injection tests were conducted over durations of 20 minutes to 2.5 days. Pressure responses were analysed using standard approaches (Cooper and Jacob, 1946) as well as fractional models (Barker, 1988) – see inset on the left.
- Thermal tracer tests were conducted through the injection of hot water and the propagation of thermal anomalies using two loops of distributed fibre-optics temperature sensing systems (FO-DTS).

Key Results – Pulse Tests

- The distribution of single-hole Transmissivity estimates appears to be binomial and range as:
  - $10^{-10}<T_{SZ}<10^{-6}$ m²/s
  - $10^{-14}<T_{PL}<10^{-8}$ m²/s

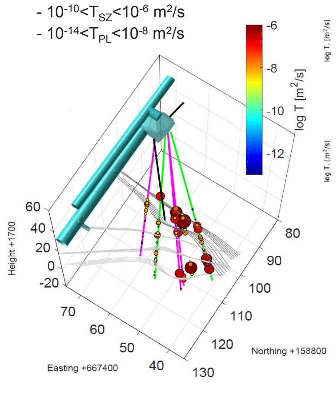

Fig. 4: 3D bubble plot showing single-hole Transmissivity values

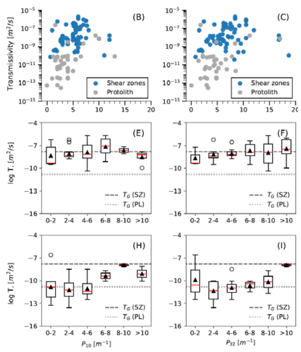

Fig. 3: Scaling of Transmissivity and fracture intensity

- Spatial correlation between high-T clusters and deformation zones (Fig. 4)
- Complex scaling with fracture intensity metrics (Fig. 3)

Key Results – Cross-hole Tests

- Normalized cross-hole pressure responses are distributed into two clusters, generally consistent with known structural domains
- Responses in the S3 shear zone (grey curves) show a strong power-law behaviour (unlike most breakthrough in S1), with a mean fractional dimension of 1.3 – see Fig 5.

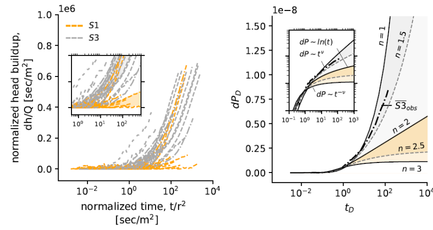

Fig. 5: Cross-hole responses (left) and mean fractional flow model (right) for our study site

- Converging pressure derivatives indicate that the flow dimension increases from n=1 to 1.5 as pressure fronts diffuse into the S1 shear zone. We interpret this as the result of the spatial integration of new forms of heterogeneities (Fig. 6).

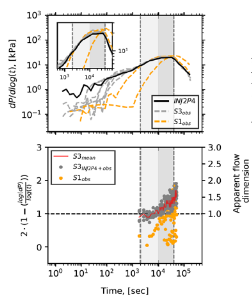

Fig. 6: Temporal evolution of the apparent flow dimension

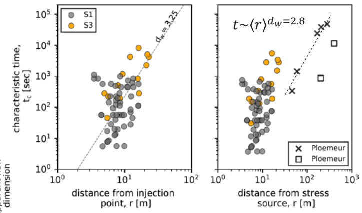

Fig. 7: Evolution of the characteristic time t_c in space (including a comparison with data obtained from a pumping test in a crystalline aquifer in Ploemeur, Brittany, carried out by other researchers (Le Borgne et al., 2004)

- Scaling exponents between the characteristic time and the Euclidean radial distance from injection are in the order of 3.2 to 3.4, i.e well above the theoretical value of 2 for normal diffusion, indicating that diffusion is anomalously slow (Fig. 7)

Key Results – Thermal Tracers

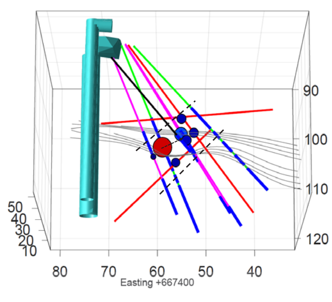

Fig. 8: 3D bubble plot showing the location of thermal breakthroughs

- Based on a 40-day thermal tracer test at 50° C, discrete thermal breakthroughs were observed along every borehole equipped with a FO-DTS system. Thermal anomalies ranged from >1°C to a maximum of 10°C about 4m from the injection point (shown in red on Fig. 8). These field results allow refining the delineation of the backbone of the fracture network and provide insights into the heat carrying capacity of fractures in granite.

Conclusions & Outlook

This study yields significant insights into the hydraulic behaviour of crystalline rocks that have similar properties to the deep reservoirs targeted for the extraction of geothermal energy in Switzerland. Here, we show that

- The permeability structure of crystalline reservoir cross-cut by shear zones is bimodal, with high-Transmissivity zones limited to shear zones
- Steady linear flow regimes develop rapidly in shear zones, even though diffusion appears to be anomalously slow (i.e. slower than expected under normal conditions where $t \sim \langle r^2 \rangle$; Using a model that accounts for anomalous diffusion yields fractal dimensions for the Grimsel Test Site and Ploemeur of 2.11 and 2.24 respectively (Acuna and Yortsos, 1995)
- Thermal tracer tests allowed refining the delineation of the principal flow paths and will be used in future studies for the parameterization of DFN models.

References

Neuzil, C.E., On conducting the modified "slug" test in tight formations, Water Resour. Res., 18(2), 1982
Cooper, H.H. and Jacob, C.E., A generalized graphical method for evaluating formation constants and summarizing well field history, EOS Trans., AGU, 27(4), 1946
Barker, J.A., A generalized flow model for hydraulic tests in fractured rock, Water Resour. Res., 24(10), 1796-1804, 1988
Le Borgne et al., Equivalent mean flow models for fractured aquifers: Insights from a pumping tests scaling interpretation, Water Resour. Res., 40(3), 2004
Acuna J. A. and Yortsos Y.C., Application of fractal geometry to the study of networks of fractures and their pressure transient, Water Resour. Res., 31(3), 1995

SCCER SoE

SWISS COMPETENCE CENTER for ENERGY RESEARCH
SUPPLY of ELECTRICITY

SCCER-SoE Annual Conference 2018

Supported by:

Schweizerische Eidgenossenschaft
Confédération suisse
Confederazione Svizzera
Confederaziun svizra

Swiss Confederation

Innosuisse – Swiss Innovation Agency

Salt Tracer Flow Path Reconstruction Using Ground Penetrating Radar

Peter-Lasse Giertzuch[1], Joseph Doetsch[1], Mohammadreza Jalali[1], Alexis Shakas[2], Hannes Krietsch[1], Bernard Brixel[1], Cédric Schmelzbach[1], Hansruedi Maurer[1]

[1]Department of Earth Sciences, ETH Zurich, Switzerland, [2]Institute of Earth Sciences, University of Lausanne, Lausanne, Switzerland

1 Indtroduction

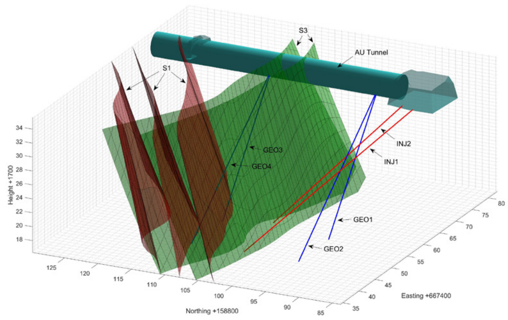

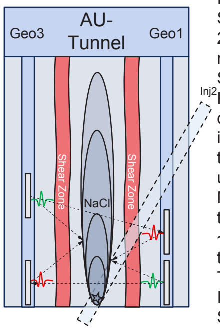

In two experiments at the Grimsel Test Site (GTS) in Switzerland, 100 L and 200 L of salt water were injected at a rate of 2 L/min in INJ2 in between the S3 shear zones, and time-lapse Ground Penetrating Radar (GPR) reflection data were recorded in GEO3 and GEO1 in the respective tests. Simultaneously, transmission data was recorded by using a 4-channel system and two 250 MHz borehole antenna sets. The temporal resolutions were ~10 min and ~30 min for the reflection and transmission acquisition, respectively. The upper figure shows the GTS with INJ and GEO boreholes, as well as the S1 and S3 shear zones. On the left the GPR survey schematic is shown.

2 Difference Reflection Imaging

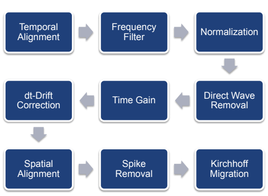

The concept of Difference Reflection Imaging relies on subtracting a reference profile that was recorded prior to tracer injection from all of the following time-lapse monitoring profiles. Only changes due to the salt tracer remain.
Left: Necessary processing steps. Below: Four differenced profiles from GEO3 at different times after tracer injection that show tracer injection, propagation, and splitting.

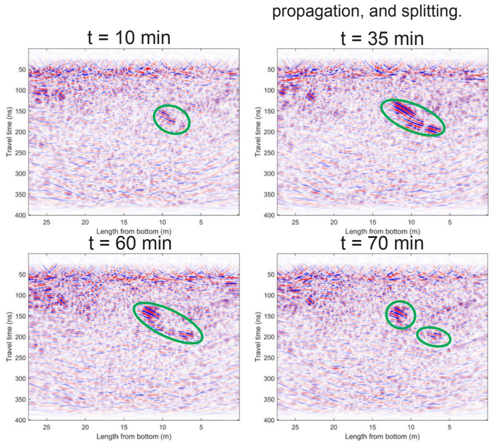

3 Difference Attenuation Tomography

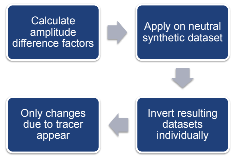

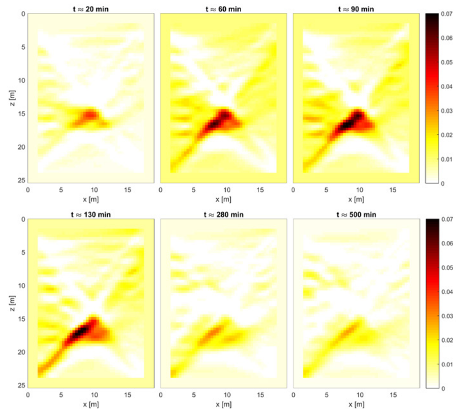

The transmission data is analyzed by a Difference Attenuation Approach. This approach allows to invert for changes due to the tracer only, disregarding all geological information in the GPR data (top). The time-lapse datasets are inverted individually and show clearly the tracer injection, build up and signal decrease in the tomography plane over time.

4 3D Flow Path Reconstruction

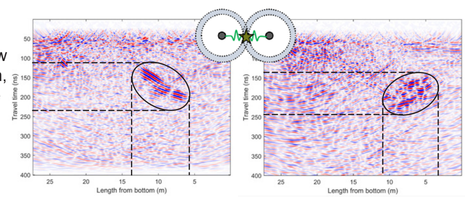

Single-hole reflection GPR data does not allow for actual localization, as the antennas show a radial symmetry. After migration, a donut shaped form contains the possible reflection locations. The data from the GEO1 and the GEO3 surveys are combined by calculating the intersections of those shapes and thereby allow for a 3D localization of the tracer. Top: The localization scheme by using the tracer locations in GEO1 (right) and GEO3 (left). Bottom left: Result integrated within the GTS model. The green ball marks the injection point, the red dots depict the tracer location. Bottom right: The results of tracer localization and inversion show good agreement.

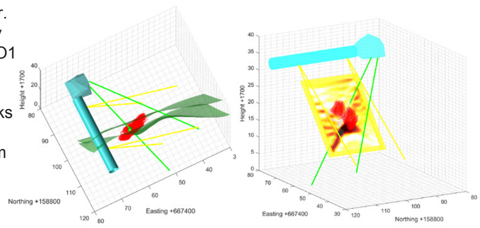

5 Combination and Verification of Results

The top figure shows that the reconstructed tracer location matches the two grey sampling intervals on the PRP lines (pink). During the test those intervals showed salt tracer breakthroughs that were recorded by STS loggers. The bottom figure shows the main breakthrough events (blue) of a heat tracer survey that was conducted in the same injection interval as the salt tracer survey (see poster by *B. Brixel*). The thermal data was recorded by optical fibers within the GTS volume. Also these points are well matched by the reconstructed location.
The reconstructed tracer flow path shows a tracer propagation within a plane between the two S3 shear zones. In a next step these results will be compared to borehole logs to identify matching fractures that seem to be responsible for the tracer flow and set up a first version of a Discrete Fracture Network, that shall be extended by combining the data with results from the thermal and conventional tracer tests.
The tomography results will be further improved by reducing the overexpression of the diagonal ray paths and in the future a Time-Lapse Full Waveform Inversion framework will be developed and applied to this data.

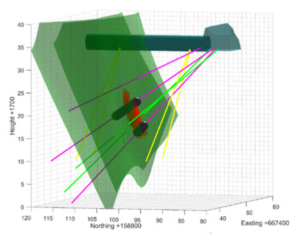

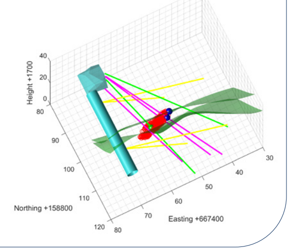

Peter-lasse.giertzuch@erwd.ethz.ch

SCCER SoE
SWISS COMPETENCE CENTER for ENERGY RESEARCH
SUPPLY of ELECTRICITY

GEO
Geothermal Energy & Geofluids

SCCER-SoE Annual Conference 2018

Comparison between DNA nanotracer and solute tracer tests in a fractured crystalline rock – GTS case study

A. Kittilä, M. Jalali, K.F. Evans, X.-Z. Kong, and M.O. Saar
ETH Zurich

Supported by:
Schweizerische Eidgenossenschaft
Confédération suisse
Confederazione Svizzera
Confederaziun svizra
Swiss Confederation
Innosuisse – Swiss Innovation Agency

Background

The DUG Lab at the Grimsel Test Site hosted an In-Situ Stimulation and Circulation (ISC) experiment (Amann et al. 2018) to investigate the key processes relevant to the development of enhanced geothermal systems (EGS). DNA nanotracer tests were conducted to i) validate and advance the application of the DNA nanotracers in decameter scale fractured rock, and ii) delineate the hydraulic features of the connected fracture volume as part of the pre- and post-stimulation characterization of the ISC experiment.
In this study (Kittilä et al. 2018), temporal moments of the DNA nanotracer breakthrough curves are compared with those of solute dye tracers, followed by the discussion on hydraulic properties of the fracture volume. The data are based on two separate tests, named Test 1 and Test 4. In Test 1, tracers were injected to borehole INJ2, and in Test 4 to borehole INJ1 (Fig. 1).

Methods

Temporal moment (TM) analysis was performed on normalized responses of the system to pulse tracer injections as age distribution functions (Shook and Forsmann 2005):

$$E(t) = \frac{C(t)\rho q_{\mathrm{out}}}{M_{\mathrm{inj}}}.$$

The *n*th TM was then calculated as:

$$m_n^* = \int_0^\infty t^n E(t)\,dt,$$

which is a measure of the tracer mass recovery (zeroth TM, M0), mean residence time (first normalized TM, M1), and degree of spreading about the center of the mass (second normalized and centralized TM, M2) (Leube et al. 2012). Furthermore, swept volume (V_P), flow/storage capacities, and the Gini coefficient (G) of the tracer responses (Shook and Forsmann 2005) were calculated.

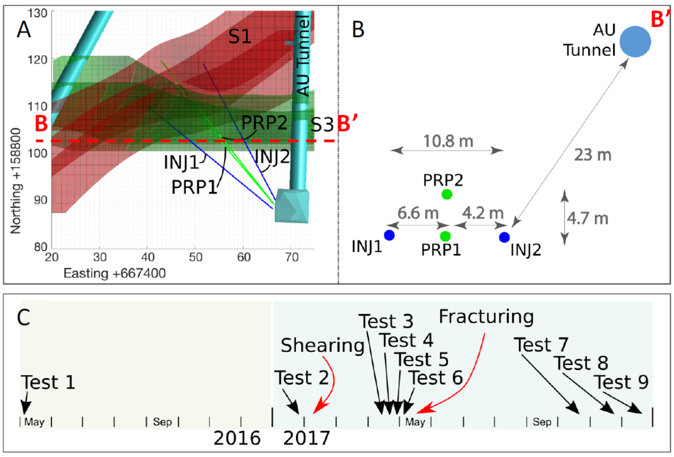

Figure 1. Visualization of two shear zones S1 and S3, the AU Tunnel, and the INJ and PRP boreholes at the DUG Lab (Krietsch et al. 2018) (A), and a sub-vertical cross-section (B-B' dashed line) showing the intersections of the boreholes and the AU Tunnel in the plane of the S3 shear zone (B). The timeline (C) shows when different tracer tests took place, in relation to the stimulation phases.

References

Amann et al. 2018. Solid Earth, 115-137.
Kittilä et al. 2018. *In preparation.*
Krietsch et al. 2018. *In review.*
Leube et al. 2012. Water Resources Research 48, W11527.
Shook and Forsmann 2005. INL/EXT-05-00400, 20 p.

Results

Table 1. Results of a temporal moment analysis from DNA nanotracers PT2 and GR-3, and solute dyes uranine (U) and sulforhodamine B (SB).

Test #	Location	Tracers	Ratio of M0	Ratio of M1	Ratio of M2	V_P (m³)	G (–)
1	AU Tunnel	PT2/U	0.99	0.71	0.39	0.36/0.50	0.32/0.36
4	INJ2 int4	GR-3/SB	0.03	0.75	0.55	0.0019/0.073	0.29/0.30
	PRP1 int3		0.09	0.41	0.42	0.0010/0.028	0.56/0.43
	PRP2 int2		0.15	0.95	1.94	0.0029/0.020	0.53/0.42
	AU Tunnel		0.10	0.78	1.02	0.060/0.72	0.39/0.33

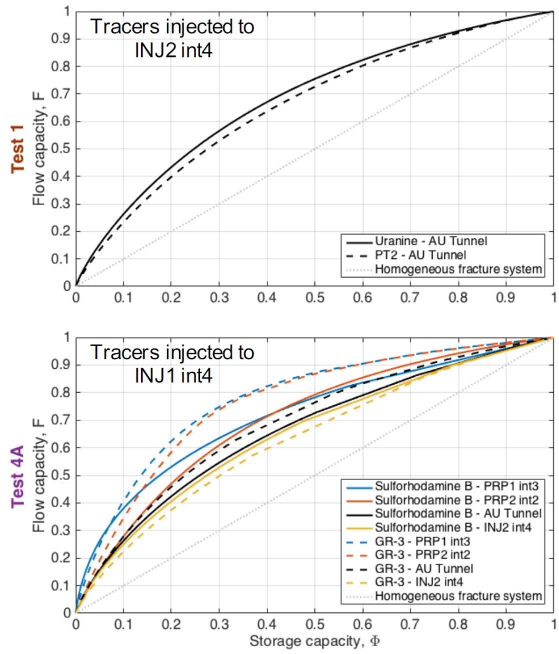

Figure 2. Flow/storage capacity diagrams from Test 1 and Test 4. Line colors indicate measurement location.

Discussion

- Tracer-based pre- and post-stimulation characterization of the DUG Lab is comprised of nine different tests (Fig. 1C), two of which (Tests 1 and 4) used DNA nanoparticles with solute dye tracers.
- Before stimulation (Test 1) only the connection between borehole INJ2 and the AU Tunnel could be studied (PRP boreholes did not yet exist).
  - DNA nanotracer and solute had almost identical recoveries, both had relatively large swept volume, and their transport was similarly distributed along that volume (Fig. 2 and Table 1).
- After shearing stimulation (Test 4) several hydraulic connections were studied.
  - DNA nanotracer had smaller mass recoveries and swept volumes from all locations, but no such trend was observed in the degree of spreading and flow distribution along the swept volume.
- The ratios of M1 (mean residence times) are not correlated with travel distance, production rate, or recovered mass.

SCCER SoE

SWISS COMPETENCE CENTER for ENERGY RESEARCH
SUPPLY of ELECTRICITY

SCCER-SoE Annual Conference 2018

Supported by:

Schweizerische Eidgenossenschaft
Confédération suisse
Confederazione Svizzera
Confederaziun svizra

Swiss Confederation

Innosuisse – Swiss Innovation Agency

GECOS

Geothermal Energy Chance Of Success

Luca Guglielmetti, Andrea Moscariello*, Schmelzbach Cédric#, Hansrued Maurer#, Carole Nawratil de Bono^, Michel Meyer^, Francois Martin^, David Dupuy°, PierVittorio Radogna°*

**Department of Earth Sciences, University of Geneva – Rue des Maraichers 13, CH-1205 Geneva*
#Institute of Geophysics, Department of Earth Sciences, ETH Zurich - Sonneggstr. 5, CH-8092 Zurich
^Services Industriels de Geneve – Chemin Chateau-Bloch 2 – CH1219 Le Lignon
°Geo2X - Rue du centre 6, CH-1377 – Oulens-sous-Echallens

Subsurface exploration for geo-energy resources production is always affected by a degree of uncertainty which reflects into the overall risk of a project
To reduce the uncertainty and the risk, industrial developers gradually collect more data to increase the accuracy and then locate drilling targets and design the drilling program (i.e. depth, amount, and geometry of the wells)

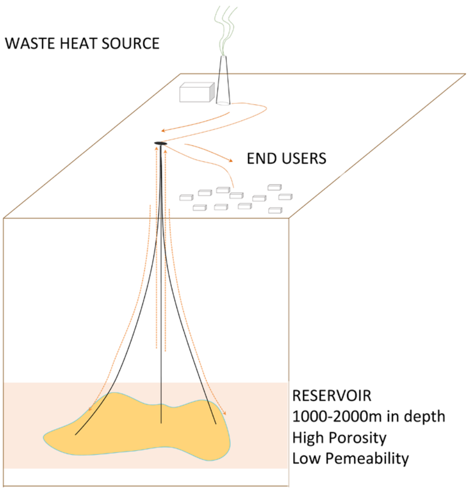

- Collecting data requires large investments which could likely to hinder the economic feasibility of an innovative projects such as in the case of UTES systems
- When the target volume is rather small (5-10km^3) such in the case of UTES, higher imaging resolution is required to properly design multiple wells to optimise the storage and production of waste heat into the subsurface.
- Finding "smart" solutions (e.g. effective and less costly) can therefore help us to achieve the required technical results to support the development of geothermal energy in the Canton of Geneva
- We intend to benefit from the fists exploration wells drileld in Geneva to develop a modular, high resolution and cost-effective geophysical data collection protocol to characterize the potential reservoir for UTES systems

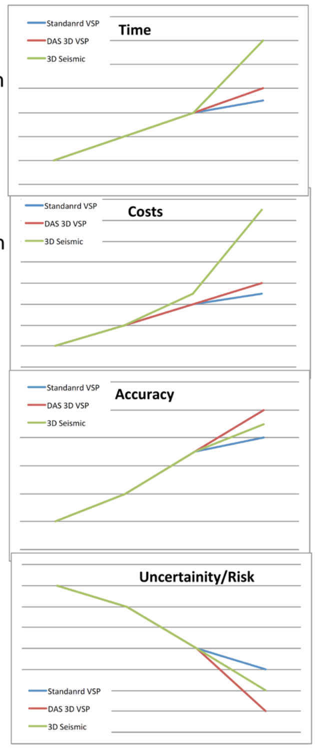

1. Quality assessment, reprocessing and reinterpretation of the available data
2. Acquisition of new gravity and S-Wave seismic data
3. Acquisition of new high resolution 2D seismic data
4. Drilling first exploration well + reservoir testing
5. Run 3D DAS VSP
6. Drill auxiliary wells + reservoir testing
7. Run additional 3D DAS VSP
8. Start Production

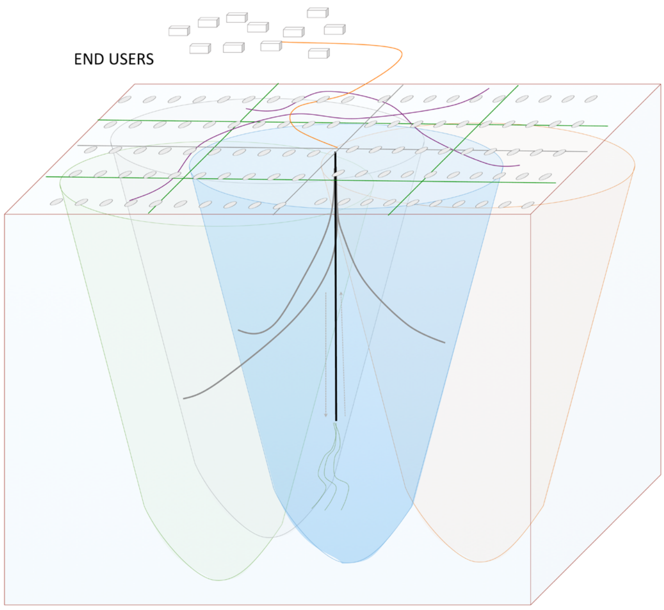

UNIVERSITÉ DE GENÈVE
FACULTY OF SCIENCES
Department of Earth Sciences

SIG

Geo2X
Geophysics for Geology

ETH zürich

SCCER SoE

SWISS COMPETENCE CENTER for ENERGY RESEARCH
SUPPLY of ELECTRICITY

SCCER SoE Annual Conference 2018

Supported by:

Schweizerische Eidgenossenschaft
Confédération suisse
Confederazione Svizzera
Confederaziun svizra

Swiss Confederation

Innosuisse – Swiss Innovation Agency

Exploring the interface between shallow and deep geothermal systems: the Tertiary Molasse.

Andrea Moscariello, Nicolas Clerc*#, Loic Pierdona*, Antoine De Haller**

* *Department of Earth Sciences, University of Geneva – Rue des Maraichers 13, CH-1205 Geneva*
# *Canton of Geneva, Service de géologie, sols et déchets,*

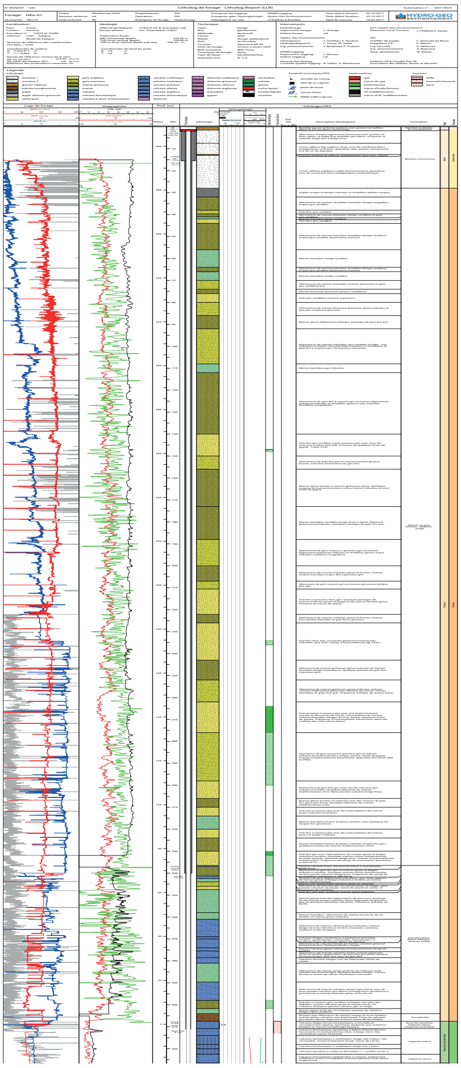

Little in known on the Tertiary Molasse succession accumulated in the Geneva foreland basin despite over the last 60 years a large amount of academic research and geo-energy exploration projects have been carried out in the Greater Geneva Basin. While the general chronostratigraphic framework and the overall sedimentology is generally known, the internal sedimentary architecture, its tectonostratigraphic significance and the reservoir characteristics (i.e. sand body and shale vertical and lateral continuity, etc.) is not yet well described.

The Molasse can play an important role while assessing the potential of deep hydrogeological budget as it could provide both storage and communication paths from the shallow ground water flows, mostly located within Quaternary deposits. and the deep Mesozoic systems, typically charged through pervasive fault systems.

A comprehensive integrated sedimentological, chemostratigraphic and structural study of this interval is under way, whose preliminary results/observations are presented here.

2D sesimc line in the western side of the Canton of Geneva where various sedimetological and structural features charcaterising the interface between the Lower Cretaceous and Tertiary units.

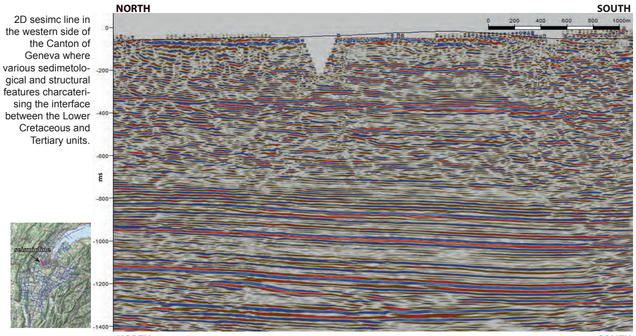

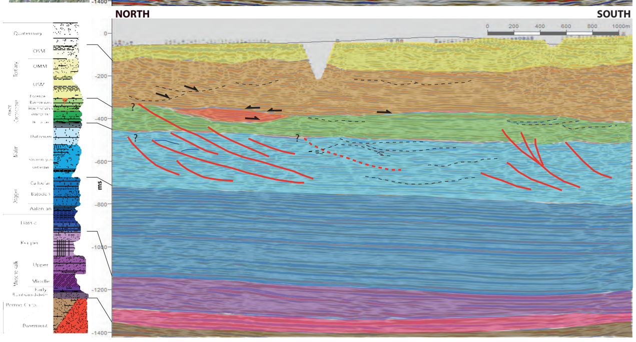

Chemostratigrahy: testing a 'new' corralation tool

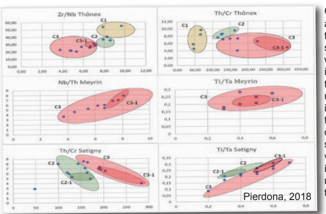

Chemostratigraphic analysis of the clastic Molasse succession penetrated in 3 wells, allows the identification of distinct stratigraphic units which increase the resolution of vertical subdivision of this thick stratigraphic interval provides better insights on its reservoir properties.

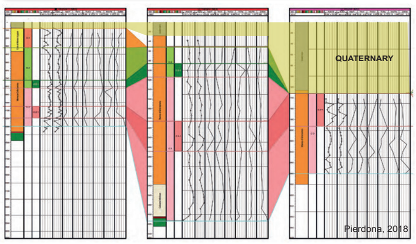

The LK-T interface

Distinct karst and open fracture network are found at the LK-T interface indicating the likely connectivity between the shallow Molasse and the deeper Mesozoic aquifers.

UNIVERSITÉ DE GENÈVE
FACULTÉ DES SCIENCES

SIG

RÉPUBLIQUE ET CANTON DE GENÈVE

SCCER SoE Conference 2018

GE-RGBA/082018

SCCER SoE

SWISS COMPETENCE CENTER for ENERGY RESEARCH
SUPPLY of ELECTRICITY

SCCER-SoE Annual Conference 2018

Supported by:

Schweizerische Eidgenossenschaft
Confédération suisse
Confederazione Svizzera
Confederaziun svizra

Swiss Confederation

Innosuisse – Swiss Innovation Agency

Processing and Analysis of Gravity data across the Geneva Basin in a Geothermal Perspective

Luca Guglielmetti, Andrea Moscariello*,*

** Department of Earth Sciences, University of Geneva – Rue des Maraichers 13, CH-1205 Geneva*

The study aims at understanding how the gravity method can contribute to the characterization of the Geneva Canton subsurface by analysing the gravity anomalies that can be associated with geological structures of geothermal interest.

Gravity is part of the solution

It has limitations, but is one of the geophysical methods that can be employed during prospection and monitoring of a geothermal site.

Higher benefits from gravity can be achieved if coupled with other exploration techniques routinely employed such as EM methods and 2D/3D seismic. The latter topic is part of the *Innosuisse* GECOS project aimed at reducing the geological risk of geothermal exploration.

Geological Setting

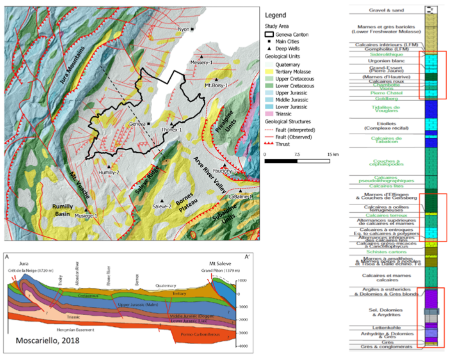

Processing of gravity public data

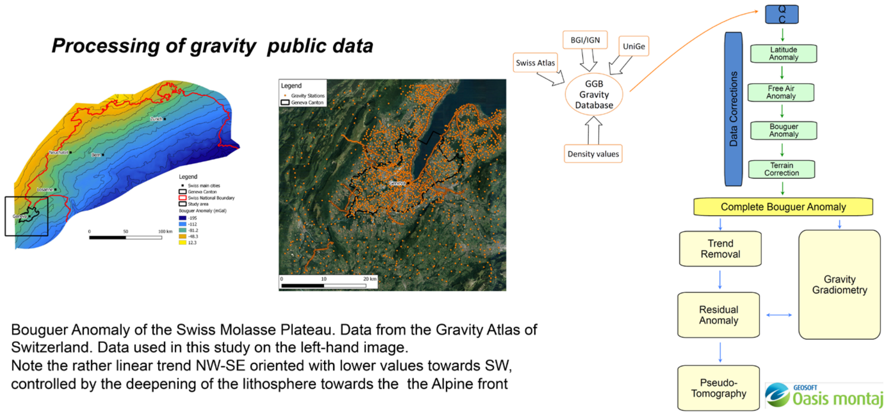

Bouguer Anomaly of the Swiss Molasse Plateau. Data from the Gravity Atlas of Switzerland. Data used in this study on the left-hand image.
Note the rather linear trend NW-SE oriented with lower values towards SW, controlled by the deepening of the lithosphere towards the the Alpine front

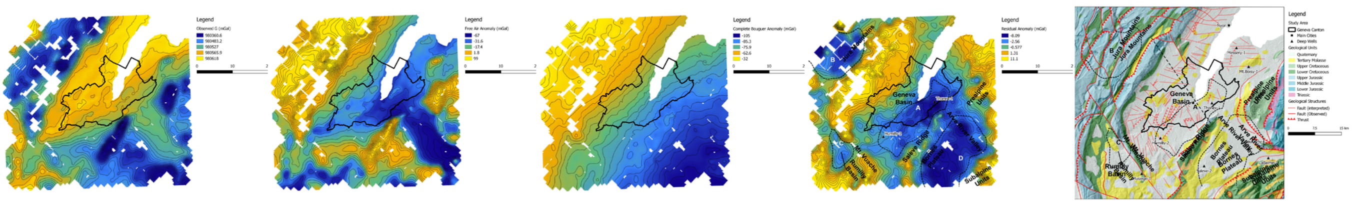

Gravity Gradiometry

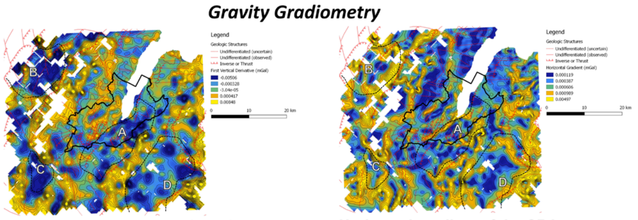

First vertical derivative of the CBA.

Horizontal gradient of the CBA

Gravity pudo-tomography:

Pseudo-gravity is based on the assumption that at increasing wavelengths correspond increasing depth of the source generating the anomaly. We tested this method by the following strategy:

- Keeping the 1km cut-off wavelengths we increased the long wavelengths to 60km
- Keeping the 60km cut-off wavelengths we decreased the short wavelengths to 1km
- We then identified qualitatively those anomalies which show significant features related to the Thickness of the main formations: Quaternary, Tertiary Molasse, Mesozoic, Permo-Carboniferous

This approach is useful to constrain the wavelength bands which can be associated with the main geological features at a certain depth range. We then used the selected wavelengths bands to run 3D forward model and Inversion on an area of geothermal interest in the Geneva Canton

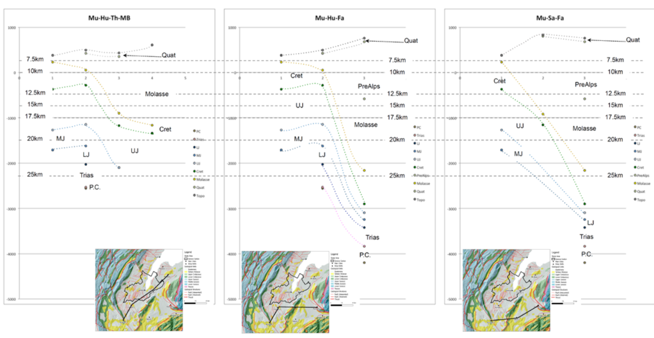

Quaternary and shallow anomaly sources in th Jura Mountains

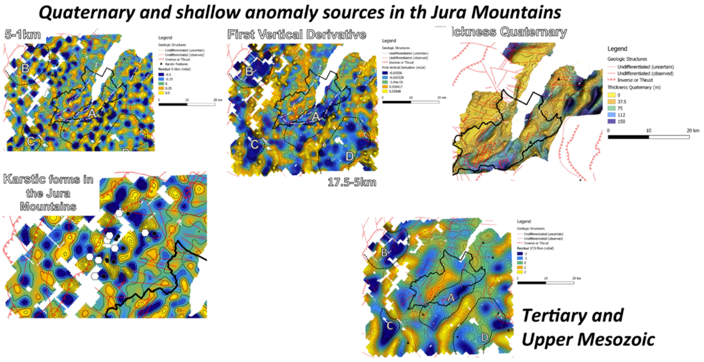

Tertiary and Upper Mesozoic

Lower Mesozoic and Deeper sources

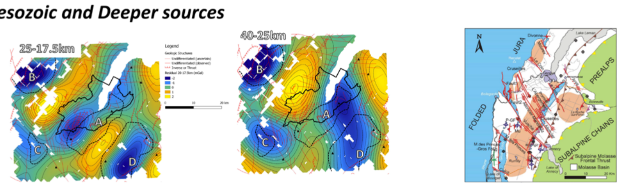

Conclusions

- Gravimetry survey is part of the exploration solution: early, cost & time effective screening of the basin (structural features at shallow to large depths)
- Comprehensive feasibility study carried out in Geneva area allows us to identify the key step processes to obtain significant results for geothermal exploration purposes in the Swiss Plateau subsurface geology.
- High resolution studies can be performed to successfully highlighting possible characteristics of major lineaments.